Control Analysis of the Action Potential and its Propagation in the Hodgkin-Huxley Model

by

Francois du Toit

Thesis presented in partial fulfilment of the requirements for the degree of Master of Science at the University of Stellenbosch

Department of Biochemistry
University of Stellenbosch
Private Bag X1, 7602 Matieland, South Africa

Supervisor: Prof J. L. Snoep

December 2010

Declaration

By submitting this dissertation electronically, I declare that the entirety of the work contained therein is my own, original work, and that I have not previously in its entirety or in part submitted it for obtaining any qualification.

December 2010

Abstract

The Hodgkin-Huxley model, created in 1952, was one of the first models in computational neuroscience and remains the best studied neuronal model to date. Although many other models have a more detailed system description than the Hodgkin-Huxley model, it nonetheless gives an accurate account of various high-level neuronal behaviours.

The fields of computational neuroscience and Systems Biology have developed as separate disciplines for a long time and only fairly recently has the neurosciences started to incorporate methods from Systems Biology. Metabolic Control Analysis (MCA), a Systems Biology tool, has not been used in the neurosciences. This study aims to further bring these two fields together, by testing the feasibility of an MCA approach to analyse the Hodgkin-Huxley model.

In MCA it is not the parameters of the system that are perturbed, as in the more traditional sensitivity analysis, but the system processes, allowing the formulation of summation and connectivity theorems. In order to determine if MCA can be performed on the Hodgkin-Huxley model, we identified all the discernable model processes of the neuronal system. We performed MCA and quantified the control of the model processes on various high-level time invariant system observables, e.g. the action potential (AP) peak, firing threshold, propagation speed and firing frequency. From this analysis we identified patterns in process control, e.g. the processes that would cause an increase in sodium current, would also cause the AP threshold to lower (decrease its negative value) and the AP peak, propagation speed and firing frequency to increase. Using experimental inhibitor titrations from literature we calculated the control of the sodium channel on AP characteristics and compared it with control coefficients derived from our model simulation.

Additionally, we performed MCA on the model's time-dependent state variables during an AP. This revealed an intricate linking of the system variables via the membrane potential. We developed a method to quantify

the contribution of the individual feedback loops in the system. We could thus calculate the percentage contribution of the sodium, potassium and leak currents leading to the observed global change after a system perturbation.

Lastly, we compared ion channel mutations to our model simulations and showed how MCA can be useful in identifying targets to counter the effect of these mutations.

In this thesis we extended the framework of MCA to neuronal systems and have successfully applied the analysis framework to quantify the contribution of the system processes to the model behaviour.

Samevatting

Die Hodgkin-Huxley-model, wat in 1952 ontwikkel is, was een van die eerste modelle in rekenaarmagtige neurowetenskap en is vandag steeds een van die bes-bestudeerde neuronmodelle. Hoewel daar vele modelle bestaan met 'n meer uitvoerige sisteembeskrywing as die Hodgkin-Huxley-model gee dié model nietemin 'n akkurate beskrywing van verskeie hoëvlak-sisteemverskynsels.

Die twee velde van sisteembiologie en neurowetenskap het lank as onafhanklike dissiplines ontwikkel en slegs betreklik onlangs het die veld van neurowetenskap begin om metodes van sisteembiologie te benut. 'n Sisteembiologiemetode genaamd metaboliese kontrole-analise (MKA) is tot dusver nog nie in die neurowetenskap gebruik nie. Hierdie studie het gepoog om die twee velde nader aan mekaar te bring deurdat die toepasbaarheid van die MKA-raamwerk op die Hodgkin-Huxley-model getoets word.

In MKA is dit nie die parameters van die sisteem wat geperturbeer word soos in die meer tradisionele sensitiwiteitsanalise nie, maar die sisteemprosesse. Dit laat die formulering van sommasie- en konnektiwiteitsteoremas toe. Om die toepasbaarheid van die MKA-raamwerk op die Hodgkin-Huxley-model te toets, is al die onderskeibare modelprosesse van die neurale sisteem geïdentifiseer. Ons het MKA toegepas en die kontrole van die model-prosesse op verskeie hoëvlak, tydsonafhanklike waarneembare sisteemvlak-eienskappe, soos die aksiepotensiaal-kruin, aksiepotensiaal-drempel, voortplantingspoed en aksiepotensiaal-frekwensie, gekwantifiseer. Vanuit hierdie analise kon daar patrone in die proseskontrole geïdentifiseer word, naamlik dat die prosesse wat 'n toename in die natriumstroom veroorsaak, ook sal lei tot 'n afname in die aksiepotensiaal-drempel (die negatiewe waarde verminder) en tot 'n toename in die aksiepotensiaal-kruin, voortplantingspoed en aksiepotensiaal-frekwensie. Deur gebruik te maak van eksperimentele stremmer-titrasies vanuit die literatuur kon die kontrole van die natriumkanaal op die aksiepotensiaal-eienskappe bereken en vergelyk word met die kontrole-koëffisiënte vanuit die modelsimulasie.

Ons het ook MKA op die model se tydsafhanklike veranderlikes deur die verloop van die aksiepotensiaal uitgevoer. Die analise het getoon dat die sisteemveranderlikes ingewikkeld verbind is via die membraanpotensiaal. Ons het 'n metode ontwikkel om die bydrae van die individuele terugvoerlusse in die sisteem te kwantifiseer. Die persentasie-bydrae van die natrium-, kalium- en lekstrome wat tot die waarneembare globale verandering ná 'n sisteemperturbasie lei, kon dus bepaal word.

Laastens het ons ioonkanaalmutasies met ons modelsimulasies vergelyk en getoon hoe MKA nuttig kan wees in die identifisering van teikens om die effek van hierdie mutasies teen te werk.

In hierdie tesis het ons die raamwerk van MKA uitgebrei na neurale sisteme en die analise-raamwerk suksesvol toegepas om die bydrae van die sisteemprosesse tot die modelgedrag te kwantifiseer.

Acknowledgements

I would like to express my gratitude to the following people and organisation:

- my supervisor, Prof Snoep, for much guidance during the project,
- Dr du Preez and especially Dr Conradie for continuing input and support,
- the financial support of the National Bioinformatics Network and
- my family, friends and Dawie for loving encouragement and support.

Dedications

To Dawie

Contents

List of Figures

List of Tables

Abbreviations

AEP	Anti-epileptic Drugs
AP	Action potential
BST	Biochemical Systems Theory
CC	Control coefficient
ECF	Extracellular Fluid
HH	Hodgkin and Huxley
HH-model	Hodgkin-Huxley Model
ICF	Intracellular Fluid
MCA	Metabolic Control Analysis
ODE	Ordinary Differential Equation
PDE	Partial Differential Equation
SB	Systems Biology
SBGN	Systems Biology Graphical Notation
SBML	Systems Biology Mark-up Language
TRN	Transcriptionally Regulated Network

Symbols

Constants as used in the Hodgkin-Huxley model

$C_m = 1\ \mu\text{F cm}^{-2}$ (membrane capacitance)

$E_{Na} = 55\ \text{mV}$ (sodium equilibrium potential)

$E_K = -72\ \text{mV}$ (potassium equilibrium potential)

$E_{leak} = -49.387\ \text{mV}$ (leak channel ion equilibrium potential)

$G_{Na} = 120\ \text{m}\Omega\,\text{cm}^{-2}$ (sodium conductance)

$G_K = 36\ \text{m}\Omega\,\text{cm}^{-2}$ (potassium conductance)

$G_{leak} = 0.3\ \text{m}\Omega\,\text{cm}^{-2}$ (leak channel conductance)

$R_2 = 35.4\ \Omega\,\text{cm}$ (axoplasmic resistance)

$a = 238\ \mu$ (membrane radius)

Chapter 1

General introduction

Centuries ago humans started to ponder the root of their intelligence, emotions and existence. In about 400 B.C. Hippocrates already discussed epilepsy as a disturbance of the brain, earning neuroscience its place as one of the oldest sciences today. Although not based on scientific evidence then, many hypotheses of the great minds have since been proven. An enormous array of significant discoveries has been made in neuroscience to date, both experimentally and theoretically, leading to vast differentiation in the field; neuropsychology, neuroanatomy, neurophysiology, neuropharmacology and computational neuroscience to name but a few.

In computational neuroscience, many neurological phenomena have been accurately described by complex models, from the behaviour of multi-neuron systems to more abstract phenomena such as consciousness. Andrew Hodgkin and Alan Huxley were at the forefront of computational neuroscience 58 years ago with their voltage clamped model describing the firing characteristics of the neuronal axon[1]. They made a valuable contribution to our quantitative understanding of the action potential (AP) in neuronal signalling, especially since the existence of membrane channels that are responsible for transferring ions across a cell membrane, was unknown. Their work was the foundation of a mechanism that is now well characterised and researched.

In the last few years, the vast diversity of biological systems and advances in technology (i.e. in the omics fields) has led to the isolation, identification and characterization of a great many, largely qualitatively described, biological components. This includes the array of ionic channels found in neuronal membranes. A plethora of mutations in genes coding for voltage-gated ion

channels has been identified affecting electrically excitable tissues such as brain, heart and skeletal muscle[2,3]. It is, however, the interactions of these components that elucidate the functional behaviour of biological systems. This is the task that the field of Systems Biology (SB) faces. Interestingly, SB and the field of computational neuroscience have managed to remain separate for a long time, even though the first initiatives in SB were led by neuroscientists[4]. De Schutter[5] indicated some reasons for this and reports that these two fields can learn from each other. Only recently have the two fields started to overlap, with Kotaleski and Blackwell[6] reporting the use of systems biology approaches in the computational neurosciences.

The importance of the use of models to accurately describe biological system behaviour has long been recognised. In computational SB, the interaction of components is mostly analysed numerically using kinetic computer models. Kinetic models allow us not only to arrive at a quantitative description of the system, but also to test hypotheses and gain understanding of the system. These models are either built in a "bottom-up" approach by using the wealth of available experimental data of biological components, or in a "top-down" approach built from observed systems behaviour, on which the model is fitted[7]. Interestingly, it is not immediately clear how to classify the approach that Hodgkin and Huxley (HH) used to construct their model. Is it a bottom-up approach since they measured the ionic conductance changes to construct their model, or is it a top-down approach since they did not use the specific kinetic characteristics of the ion channels? This question will be addressed in more detail in chapter 4, after an in-depth analysis of the model in chapter 3.

Many biological systems exhibit simple dynamic behaviour and will reach steady-state if they are kept in a constant environment. For the quantitative analysis of such steady-state systems, a mathematical framework called metabolic control analysis (MCA) exists[8–10]. This framework has often been applied to metabolic systems where it has addressed important issues like rate-limiting steps, and differences between regulation and control. Importantly for SB studies, the framework makes it possible to relate systemic properties to the characteristics of its components. This SB tool which allows us to quantify the component contribution in describing system behaviour has, however, not yet been used in the field of computational neuroscience, particularly in the observed properties of the AP.

Therefore, in this thesis: "Control Analysis of the Action Potential and its Propagation in the Hodgkin-Huxley Model", the applicability of

MCA for the analysis of the AP will be tested by first applying the recently developed extension of MCA for dynamic systems to the HH-model and subsequently addressing the question: What are the qualitative and quantitative contributions of the components of the HH-model in describing the high-level behaviour of the AP?

We start with background information in Chapter 2 on topics of importance to the work presented in this thesis.

Chapter 3 will show the results of our analysis, comparing model simulation to experimental perturbations of model components (i.e. inhibitor titrations), taken from literature. We also show the contribution of the ionic currents in bringing about the observed global change after a system perturbation.

In Chapter 4 we will also discuss our simulation results, again compared to experimental results from literature, in terms of higher-level neuronal behaviour; in particular the mechanisms associated with epilepsy.

Chapter 2

Background

2.1 Introduction

This chapter will give an overview of the status of the topics covered in this thesis, moving from a general description of the topic towards a more focussed part that has a direct link to the work. We will start with SB, giving a general description of the nature and challenges of SB, the nature and reconstruction of networks and metabolic engineering. This is followed by the introduction of a SB tool, namely MCA which is referred to both in terms of steady-state systems and dynamic systems. Then a brief discussion of neurobiology and neuroscience including why they have remained separate from SB for so long is presented. This is followed by a general introduction to computer modelling, including some model types and areas of modelling to illustrate the diversity of modelling approaches. There will then be specific focus on neuroscience in terms of the biology and the modelling of neuronal signalling, with emphasis on the HH-model. The final section in this review will focus on the mechanisms behind abnormal behaviour of the AP and how this is thought to lead to associated pathologies like epilepsy.

As humans, we are fully aware of the important role that the nervous system plays in our body. The central nervous system consists of the brain and the spinal cord, while the peripheral nervous system consists of sensory neurons and nerves connecting clusters of ganglia to each other and to the central nervous system. Whether we are awake or asleep, this system is constantly working, providing us with crucial support by performing the necessary functions. It does this through a network of interconnected neurons, including peripheral motor nerves that control our actions. The brain controls

the organs and systems of the body, either by activating muscles or by causing secretion of chemicals such as hormones. Neurons communicate with each other through signals, called APs. Mutations or changes in the neurons in our nervous system can lead to a range of pathologies, of which epilepsy is one example. A large part of the functioning of the brain is still a mystery to us and although some pathological mechanisms have been characterised to result in a change in neuronal signalling, many of these mechanisms are still unknown.

With advances in genome sequencing, the full range of components in biological systems can be identified. Effectively, this means that all possible components can be characterised, which has interesting implications for the modelling approach and SB: component information can be used to construct a model from component characteristics, which should make it possible to give a complete and accurate description/prediction of high-level system behaviour.

2.2 Systems Biology

2.2.1 An overview

Biologists have always tried to improve their understanding of organisms by gaining knowledge about (or insight into) how organisms function, via investigating progressively smaller details (components) of those organisms. A different trend started to appear where they searched for emergent properties by studying the interaction of these components. Although this approach might have been new to biology at the time, it was not to scientists in other fields of research. In 1948, the founding father of cybernetics, Norbert Weiner, already considered technical and biological systems as objects for the same scientific approach[11]. One of the first numerical simulations in biology was of a neuronal model describing a cellular function emerging from interactions between components. This model was constructed in 1952 by Alan Hodgkin and Andrew Huxley[1], which, being one of the first numerical simulations in biology, is now seen as the beginning of computational SB[12]. In 1966, the formal study of SB as a distinct discipline was launched by systems theorists Mihajlo Mesarovic[13] and Ludwig von Bertalanffy[14].

It was around that time and soon after that other attempts were made, though still under the name of cybernetics, keeping the idea of the study of *component interaction* alive. An example is biochemical systems theory

(BST). BST is a mathematical modelling framework for biochemical systems developed in the late 1960s by Michael Savageau and others, based on ODEs in which biochemical processes are represented using power-law expansions in the variables of the system[15,16]. BST is similar in formalism to MCA (Section 2.3), but with different objectives. In BST the analysis is made in terms of variables and it is a more general approach overall, whereas in MCA the analysis focuses on the processes. MCA is more appropriately used in studying enzyme kinetics to address questions such as: to what extend does a reaction control the steady state flux?[8,9]

It has been a long-standing goal of biological sciences to reach a system-level understanding of biological phenomena. The 1980s saw the thriving of molecular biology as well as scepticism about theoretical biology. As far as molecular biology was concerned, only phenomenological analysis was possible, which made a system-level understanding somewhat unattainable. This caused the quantitative modelling of biological processes to become less popular. However, the birth of functional genomics in the 1990s meant that large quantities of data became available. With the completion of genome projects and an increase in the amount of data available from genomics, transcriptomics and proteomics, increased computing power, developments in measurement precision and the understanding of gene regulation, it became possible for system-level analysis to be grounded on understanding at a molecular-level[17], which led to more realistic models. In 2000 SB emerged as a field in its own right.

SB was henceforth a biology-based interdisciplinary science that uses a holistic perspective and focuses on the study of complex interactions between components of biological systems. More specifically, it involves the reconstruction of dynamic systems from the quantitative properties of their elementary building blocks. One aim of SB is to overcome the deficiencies of current models by creating fully dynamical models. The way to deal with these deficiencies can generally be divided into two approaches (see Section 2.5.1 also). One group of researchers prefers to supplement them through an integration of data from different levels and sources[18] (bottom-up approach), the other to shift the focus from the elementary components of biological processes to *systems* of elementary components[19,20] (top-down approach). Both approaches bring together scientists from a variety of disciplines, such as biology, systems theory, computer science, physics, chemistry and interdisciplinary areas of applied science like the development of measurement

instruments.

2.2.2 The challenges

Requirements for a system-level understanding

Although a system consists of identifiable, tangible matter like genes, proteins and other molecules, the higher-level system behaviour might seem less tangible at first glance. This is why a *system-level understanding* is somewhat vague and hard to define. Nonetheless, there are four important phases that will lead us to a system-level understanding.

First, the structure of the system must be known. Although it is still a static view of the system, it is an important first step. Structure is divided into both physical and interaction structure. Interaction structures include gene regulatory networks and biochemical networks that identify how components interact within and between cells. Physically, details of a specific region of a cell or overall structure of a cell are important as they may impose constraints on possible interactions. The network interactions have to be known both qualitatively and quantitatively. Secondly, the system dynamics of these interactions must be well characterised. Third, methods to control the system must be explored. An understanding of control of the system via the intrinsic dynamics of the cell enables us to design drug compounds according to specific molecular targets. Lastly, as an end result, one would have a rational tool for constructing a designed and modified system.

The cell is constantly bombarded with changes in its immediate environment. The ability of the cell to deal with these changes by employing a range of strategies is referred to as robustness. As robustness is a system-level property, the abovementioned phases that lead to a system-level understanding are imperative to give us insight into the mechanisms underlying robustness. Also, the specific aspect of the system, the function to be maintained, and type of perturbation that the system is robust against must be well-defined in order for us to make solid arguments regarding the strategies employed by the cell.

Robustness

Robustness is a fundamental feature that is observed across a range of species and biological systems. It is a property of the system that allows it to

maintain a specific function despite perturbations, like a change in temperature or nutrient availability. Robustness is, amongst others, responsible for bacterial chemotaxis[21–23] and tumour resistance against therapies[24,25]. Because robustness seems to be present everywhere, there may be a universal basis of principles for it which may lead to opportunities for finding cures for complicated diseases such as cancer and diabetes. Robustness is a system-level property and cannot be observed by merely examining the system components. Also, diseases may be the result of trade-offs between robustness and fragility. Thus it comes as no surprise that one of the themes in SB is to understand robustness in biological systems, its trade-offs and the underlying principles[26].

Across biological systems there are common mechanisms that are responsible for system robustness. They include extensive system control in the form of negative feedback loops which ensure that even dynamic systems remain constant (of which bacterial chemotaxis is an example[21–23]), modularity which isolates a perturbation from the rest of the system[27–30], and alternative mechanisms which increase tolerance against component failure by providing alternative methods to maintain a function of the system despite the perturbation, of which phenotypic plasticity is an example[31,32].

Apart from the abovementioned requirements, the ensuing model construction and analysis of the system produces its own stumbling blocks, for example the standardisation of model representation.

A standardised platform for Systems Biology

For effective theoretical analysis, a useful standardized platform for model representation is needed. To this end, standardisation techniques, such as Systems Biology Mark-up Language (SBML), Systems Biology Graphical Notation (SBGN) and Minimum Information Requested In the Annotation of biochemical Models (MIRIAM), were developed and play an important role in the software platform of SB. These technologies will briefly be mentioned below. Note that the standards mentioned here are not a complete list, but are rather intended to serve as example of what is available.

SBML, SBGN and MIRIAM As stated, SBML (http://www.sbml.org/) was designed to enable standardised representation of models and facilitates the exchange of models among software tools that comply with these standards[33]. SBML is a tool-neutral, computer-readable format for representing

models of biochemical reaction networks, which makes it applicable to metabolic networks, cell signalling pathways, genomic regulatory networks, and other modelling problems in SB[33]. This project started in 1999 and is widely supported by the SB community. SBML is based on XML, which is a standard medium for representing and transporting data that is extensively used on the Internet, as well as in computational biology and bioinformatics. The fact that SBML is tool-independent, makes model transportability, reuse, publication, and survival possible[34].

Another standardisation effort, SBGN (http://www.sbgn.org/), is a solidly defined system that is aimed at the formation of standard graphical representations of molecular interaction networks[35].

Many of the published models in biology are not made available or are insufficiently characterised for reuse. As a result, a set of rules for curating quantitative models of biological systems have been created. These rules, collectively termed MIRIAM, define procedures for encoding and annotating models that are represented in machine-readable form[36].

Model repositories The standardised models are encoded and stored in public databases, such as EcoCyc[37], the CellML repository*, JWS Online[38], RegulonDB[39] and BioModels database[36,40]. The BioModels database, for instance, developed through an international collaboration between the SBML team (US/UK/Japan), EMBL-EBI (UK), DOQCS (IN) the Keck Graduate Institute (US), Systems Biology Institute (Japan), and JWS Online (South Africa), provides access to published peer-reviewed quantitative biological models.

2.2.3 Reconstruction of networks

As mentioned previously, the development in genome sequencing and other experimental technologies makes it possible to reconstruct complex networks of interacting cellular components at a system-wide level[41–44]. A goal of SB is to develop theoretical models with which to describe and predict cellular behaviour at a whole-system level.

The macroscopic structures of the biological networks, which are uncovered by analysis of a network as a whole, can identify system-level principles/rules governing the organization of interacting cellular components. Although these

*http://www.cellml.org/examples/repository/

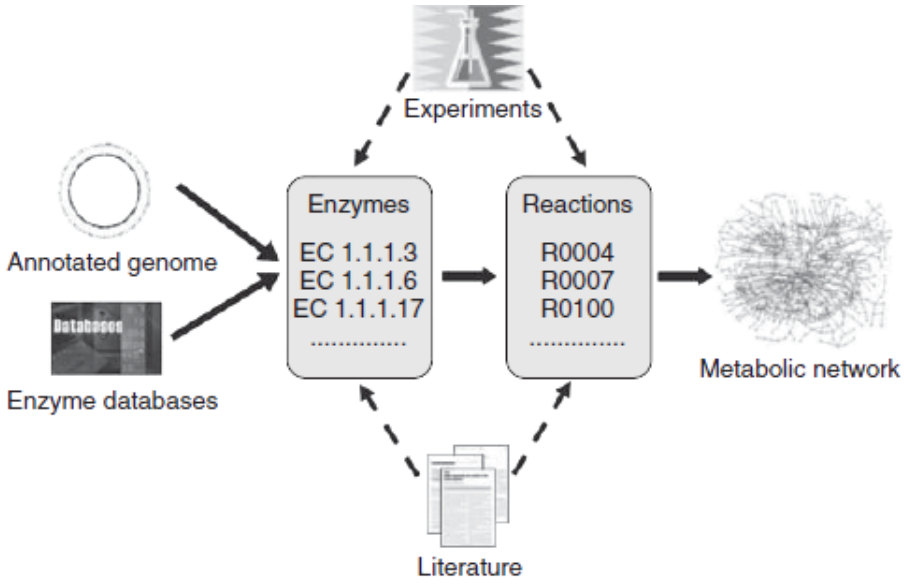

Figure 2.1: Processes to reconstruct metabolic networks. The high-throughput method (indicated by the solid arrows) allows the direct reconstruction of an organism-specific metabolic network from genome or enzyme databases. Additionally, new enzymes or reactions from biological experiments or literature (indicated by the dashed arrows) can be added, obtaining high-quality metabolic networks. The scheme was taken from *Introduction to Systems Biology* by Ma et al. (2007)[45].

structural properties still give only a static picture of the whole system, they can serve as a basis for analysing the dynamic behaviour of the network (e.g., information and material flows), which is the next necessary and more demanding step in network analysis[45].

In this section, there will be a brief focus on network reconstruction, specifically in metabolic networks and transcriptional regulatory networks.

Genome-based reconstruction

Organisms have differing enzyme pathways in their metabolic networks which influence their metabolic ability to take up substrates or produce metabolic products. However, fully sequenced genomes and gene function annotation methods based on sequence similarity allow us to reconstruct metabolic networks which are organism-specific and are based on the genome alone[46–48]. The method to reconstruct a metabolic network is illustrated in Fig. 2.1. It is thus possible to use the genome sequence of a newly sequenced organism directly to construct a list of enzymes included in its metabolic network, without having to do many biochemical experiments to study the metabolic

enzymes[45].

High-quality reconstruction

The above mentioned (high-throughput) reconstruction method is necessary for the comparative analysis of large-scale networks, as it allows the network reconstruction of many organisms simultaneously. However, there is a trade-off between high productivity and high quality. Networks constructed in a high-throughput manner are at risk of not being complete. This is due to a couple of reasons:

1. Non-enzyme-catalysed reactions exist that occur spontaneously in a metabolic network - they have to be added to this network to avoid missing links in the network.

2. The functions of a large part of the genes in a genome are not known; many experimentally determined enzymes (which catalyse reactions) are not found in any fully sequenced genomes. This is reflected in the KEGG database, where half of the enzymes are not coded by any gene[45].

There are also discrepancies between the networks in different databases, like KEGG, ExPASy and EcoCyc[37], for even the best-studied organisms like *E. coli*. This is why human curation of these networks is needed as well as literature surveys to verify and correct gene-enzyme relationship data. These network quality improvement processes are, however, time-consuming, hence high quality metabolic networks are only available for a small number of organisms, like *E. coli* and *S. cerevisiae*[41,49–51].

Transcriptionally regulated network reconstruction

Although a metabolic network of an organism represents a picture of the possible reactions in it, this picture is static, while in reality not all of these reactions occur in the cell at the same time. The enzymes in a pathway for specific substrate uptake, for example, are only induced when the substrate is present. In prokaryotes enzyme induction is mainly controlled by the transcriptionally regulated network (TRN). These network interactions are between transcription factors and target genes. As transcription factors activate or repress gene expression, it would be useful to reconstruct the TRN to obtain a better understanding of the dynamic regulation of metabolic networks. However, the reconstruction of a genome-scale TRN is not as easy

a task as the sequence similarity–based, high-throughput metabolic network reconstruction[52]. Again, genome-scale TRNs are only available for well-studied organisms. Several databases have been developed which store and manage the curated regulatory interaction information from literature. RegulonDB[39] is a major database for the *E. coli* regulatory network, DBTBS[53] for *B. subtilis* and Prodocir[54] for prokaryotes. TRANSFAC[55] contains information on eukaryotic, though mainly yeast, transcription factors and their genomic binding sites. Because the information in each database is often not very complete, it is useful to integrate the information from different databases to acquire more complete networks.

An integrated network

Not only is gene expression under transcriptional regulation (which ultimately controls the metabolic fluxes), but the effect of transcription factors on genes can be modulated by the concentration of certain metabolites which can bind to them. Consequently, in order to improve our understanding of metabolic regulation in a cell, integration of the different possible interactions seems necessary to obtain the whole picture. Various studies on the integration of cellular interactions for network structure or functional analysis have been published[56,57]. As an example, Ma et al.[42,58,59] are in the process of constructing networks of all the available interactions in *E. coli*, including transcriptional regulation (between transcription factors and their target genes), metabolic reactions (between metabolites), metabolite-protein interaction (between metabolites and transcriptional factors) and protein-protein interactions (including signal transduction). This allows novel conclusions which cannot be revealed through individual network analysis alone[45].

2.2.4 Metabolic engineering

Cells require substrates to supply them with free energy, create precursor metabolites needed to fuel cellular processes and ultimately, for growth and maintenance. The substrates are converted through reactions catalysed by enzymes. Collectively these processes are known as metabolism. The arrival of the post-genomic era and genome sequencing has made the identification of the elements of the cellular inventory possible. It has allowed us to answer questions such as which genes are in the genome, which proteins they encode for

and what their functions are. It has also led to the development of large-scale analytical techniques allowing us to quantify the metabolic state (metabolic fluxes) in a cell at a given time. When the cellular inventory is viewed as a network of interacting genes, proteins and reactions, it is possible to break down the cellular complexity and represent the cell as a simplified system that can be used to relate genotype and phenotype. It is this integration of structural networks with quantified molecular and metabolic elements that has been termed SB[20,60,61]. SB is used as a framework to develop models and tools to explore the emergent properties and capabilities of microbial systems, to explore hidden regulatory mechanisms and to design superior strategies for producing microbial cell factories with desired phenotypes[62].

Data analysis

The exploration of these complex systems persistently involves the analysis of data. There are, however, a number of data analysis techniques and predictive tools available which help facilitate this process. Again, the methods discussed here are only an example of what is available.

Classical methods Due to intrinsic biological variability, fold change cannot be used as an indicator of significance of differential mRNA or protein expression. An alternative would be to run biological replicates and to apply statistical test to identify significant changes[63,64]. For a simultaneous comparison between two datasets, tests often used are analysis of variance (ANNOVA) or multivariate analysis of variance.

Principal component analysis (PCA) is a method for reducing dimensionality which allows us to visualise high-dimensional data in a low-dimensional space. PCA breaks the high-dimensional space down into a space of n dimensions, where n refers to the number of principal components. This allows the projection of omics-data onto a plane so that the variables, like mRNA transcripts, can be located close to each other[62].

Clustering is the most prevalent method for grouping profiles of "omics" data. Using gene expression data as example, clustering would group genes based on their similarity profile[65]. Genes sharing a common profile will cluster together and are further treated as such. Clustering is therefore also seen as a way of reducing dimensionality[62].

Integration is the key Clustering and PCA are essentially data driven by searching for hidden correlations in the data, using data alone. The premise behind these methods is that co-regulated genes show similar expression patterns. It is, however, assumed that there may be an all-all interaction amongst genes being analysed, making these data-driven methods sensitive to noise in the data as there is a high degree of freedom. As a result, weak, biologically significant correlations may be overshadowed by strong, biologically insignificant, correlations. A way to overcome this is to reduce the degree of freedom during data analysis. This can be done by the integration of "omics" data with known biological interactions that occur in the cell, like protein-protein interaction networks or metabolic networks.

Thus, if we want to know how the flux control is exerted at different levels of cellular regulation we have to understand the principles and architecture of the regulatory machinery at its different levels. There are several integrative techniques, of which two will briefly be mentioned. Ideker et al.[66] introduced an integrative approach where the search for highly transcriptionally co-regulated sub-networks in molecular interaction networks is aimed at uncovering modules of cellular transcriptional regulation resulting from a genetic or environmental perturbation. A similar approach was used by Patil and Nielsen[67] in which they used the integration of gene expression data of the metabolic network to uncover transcriptional regulation of metabolism. In this case, the metabolic network was represented as a graph where enzymes are connected if they share common metabolites. Thus the resulting high-scoring sub-network corresponds to the most highly correlated (and connected) enzymes reflecting, at a transcriptional level, the propagation effects of a genetic or environmental perturbation on metabolism.

2.3 Traditional MCA and MCA for dynamic systems

MCA[8–10] is a mathematical framework that has as one of its motivations a quantification of how the system variables (such as flux through a metabolic pathway or metabolite concentrations) change in response to parameter variations (such as enzyme concentrations). Traditionally, control coefficients express how these variables are dependent upon the parameters. Control coefficients are thus defined as the % change in a steady-state variable, x,

upon a 1 % perturbation in the activity of an independent process, v_i[68]. In general

$$C^x_{v_i} = \frac{\partial \ln x}{\partial \ln v_i} = \frac{\partial x}{x} / \frac{\partial v_i}{v_i}. \tag{2.1}$$

An important property of control coefficients is that, for any flux, the control coefficients of all the processes within the system sum to one (the flux-control summation property) and, for any concentration, the control coefficients of all the processes within the system sum to zero (the concentration-control summation property). This is expressed mathematically as

$$\sum_{i=1}^{n} C^J_i = 1, \tag{2.2}$$

$$\sum_{i=1}^{n} C^s_i = 0. \tag{2.3}$$

In agreement with the summation theorems, the notion of a rate-limiting step in metabolism is replaced with one which describes the control on a system property to be shared between the processes in a system. In addition to control coefficients, elasticity coefficients quantify to what extent the rate of an independent process in a system is changed immediately upon a change of any molecular species or parameter that affects that process directly. Parameter elasticity coefficients can operationally be defined as the % change in a reaction rate, v_i, upon a 1 % perturbation of a parameter, p, for the isolated reaction and is expressed as

$$\varepsilon^{v_i}_p = \frac{\partial \ln v_i}{\partial \ln p} = \frac{\partial v_i}{v_i} / \frac{\partial p}{p}.$$

A further relation of the elasticity coefficient and control coefficient where the kinetic properties of individual reactions and the system properties of a pathway can be expressed, is known as the response coefficient. Through the response coefficient it is possible to describe the effect that a change in a parameter of a reaction, p, has on a steady state variable of the system, x. Response coefficients are mathematically expressed as

$$R^x_p = C^x_{v_i} . \varepsilon^{v_i}_p = \frac{\partial \ln x}{\partial \ln v_i} . \frac{\partial \ln v_i}{\partial \ln p} = (\frac{\partial x}{x} / \frac{\partial v_i}{v_i}) . (\frac{\partial v_i}{v_i} / \frac{\partial p}{p}) = \frac{\partial x}{x} / \frac{\partial p}{p}. \tag{2.4}$$

MCA is mostly used to analyse time-invariant properties of steady-state systems. Traditional MCA could not be used to analyse dynamic systems, where temporary or permanent variations of metabolic fluxes and concentrations are significant (this also entails that the connectivity theorem is only valid to describe steady-state systems and is not defined for dynamic systems).

One of the first extensions to traditional MCA to allow the description of dynamic systems, was to introduce a time-dependent control coefficient, which would enable MCA to describe dynamical systems[69]. This formulation could, however, not be generalised to all dynamic systems as the magnitude of time-dependent control coefficients, describing autonomously oscillating systems, diverge as time progresses[70,71]. Also, extensions to standard MCA proposed by Heinrich and Reder[72] cannot be generalised to all dynamic systems as the concentrations of metabolites are not necessarily in the vicinity of a steady state[70,71]. Acerenza and Kacser[73,74] analysed the control properties of time-invariant variables with dimensions of time (for example relaxation time and period of oscillation) and deduced summation theorems for them.

Until recently, it has not been possible to quantify the control that each reaction step of a dynamic system plays in regulating fluxes and metabolite concentrations. Nonetheless, Conradie et al.[75] showed how time-dependent flux and concentration control coefficients can be determined for dynamic systems, when the time domain is treated as percentage progression through any arbitrary fixed interval of time. They also showed that steady-state flux and concentration control summation theorems hold for dynamic systems[75].

2.4 Neurobiology and neuroscience

The term neurobiology is often used interchangeably with neuroscience, although the former refers to the biology of the nervous system and the latter to the entire science of the nervous system. Neuroscience is currently an interdisciplinary science that involves other disciplines such as psychology, statistics, physics and medicine. A range of different approaches thus exists to study the structural, functional, molecular, computational and medical aspects of the nervous system.

Recent theoretical advances in neuroscience have been aided by the use of computational modelling of neuronal networks. Theoretical and computational neuroscience, in which the HH-model originated, is but one of the many branches of neuroscience and links the diverse field of neuroscience

with computer science. Computational neuroscience uses computational approaches to investigate the properties of nervous systems at different levels of detail, for instance focussing on the description of functional and biologically realistic neurons and neural networks and their physiology and dynamics[76,77]. Apart from the computer simulation of numerical models, the experimental verification of these models is also of importance[78].

2.4.1 Neuroscience meets Systems Biology

Since one of the main focus points of this thesis is MCA and its use in our analysis of a neuronal model, it seems relevant to focus on the relationship between computational neuroscience and SB.

Despite the fact that one of the early initiatives in SB was lead by neuroscientists[4], the field of SB seems to have gone its own way in terms of development. There are a few possible reasons as to why the fields have grown apart, one of which perhaps lies in the difference in the respective cultures with regard to data driven modelling: where SB is faced with a data-rich environment and the challenge is to separate the important from the less important rather than to infer the unknown, neuroscience is usually faced with incomplete data and a lot of guesswork has to be done. There also seems to be a difference in interest among the two groups: systems biologists often think of computational neuroscience work as being too specialized, while in turn, computational neuroscientists seem to have little interest in molecules and genes[5].

Be that as it may, the two fields have a lot to offer each other. Neuroscience is a more mature field than SB and thus has more experience in some specialised topics[79], for instance a strong acquaintance with simulator software development for multi-scale modelling. However, since neuroscience specific programs, like the Human Brain Project[80] were brought to an end, it seems that there will be increasing pressure on those computational neuroscientists modelling at cellular levels, to cross over to the world of SB. In the past few years, there were some software developments that combine computational neuroscience and systems biology techniques, but this integration has only started recently.

According to De Schutter[5] it is unsure whether this will happen in the future, but it is fair to say that the two fields could and should learn from each other. In Chapter 4, we will focus on using our model predictions

(from Chapter 3) to see how MCA can be helpful in understanding abnormal behaviour of the AP, brought about by mutations in neuronal membrane channels. This is already a step in the right direction, as we are using a SB tool (MCA) to improve our understanding of a system described by a computational neuroscience model (the HH-model). Let us, however, first introduce the field of modelling, specifically the construction approach, mathematical modelling and areas of modelling.

2.5 Modelling and model construction

The concept of modelling has existed for a long time and is used in various fields, but usually with more or less the same outcome in mind - that of facilitating the understanding or prediction of a system or certain system behaviour. The emergent properties of biological systems are excellent examples of behaviour brought about through the complex interplay of simpler, integrated components. Traditionally, reductive methods were used in the study of biological systems, in which quantities of data were gathered by category, i.e. concentration over time in response to a certain stimulus. Computers are critical to the analysis and modelling of data. The eventual goal is to model, accurately and in real-time, a system's response to environmental and internal stimuli, for example a model of a cancer cell in order to find weaknesses in its signalling pathways, or modelling of ion channel mutations to see the effects on neuronal signalling and even on a beating heart.

The mathematical model is probably the most widely used type of model because it can take many forms, including but not limited to dynamical systems, statistical models, differential equations, or game theory models. Also, these and other types of models can overlap, resulting in a model that includes a variety of abstract structures. They can thus be used not only in the natural sciences (i.e. physics, biology, earth science, meteorology) and engineering, but in the social sciences as well (i.e. as psychology, sociology, political science and economics), although mathematical models are used most comprehensively by physicists, computer scientists, economists and engineers[81].

Various fields in the biological sciences, from ecology and epidemiology to medical fields like virology and neurology, rely on models to test hypotheses through model prediction. But first, an important aspect that has to be considered carefully is what approach to take in constructing the model. In

this section, two different approaches to construct a model will be mentioned, follwed by a discussion on mathematical modelling, after which the focus will be on some examples of modelling in biology with a specific focus on the neurosciences.

2.5.1 Construction approach

A model consists of low-level components acting together to display high-level system behaviour. When constructing a mathematical model of a biological system, generally two different approaches exist: that of "top-down" and "bottom-up". The bottom-up approach uses detailed information (experimental data) about the components and their interactions. This information is used to inspect the mechanism through which system behaviour or a property emerges. Therefore these models do not attempt to fit the model on system behaviour, but they can be used to make predictions about the behaviour of the system. In contrast, the top-down approach uses measured or observed details of the system behaviour to construct the model. What approach is taken thus depends on the type of data available as well as the purpose of the model. In the bottom-up approach, system behaviour is used only for model validation[7]. The wealth of available genomic data makes the bottom-up approach extremely feasible by allowing the use of component data in model construction. Some models are constructed using a combination of bottom-up and top-down approaches.

2.5.2 Mathematical modelling

As mentioned above, the preference of what type of model is to be created lies in the data available, the components being studied and the desired outcome of the model. A diverse spectrum of modelling approaches exists that range from more abstract, such as models that include protein interaction graphs, to highly concrete, like models containing differential equations.

In 1974 Pieter Eykhoff defined a mathematical model as a representation of the essential aspects of a system presenting knowledge of that system in a usable form[82]. A mathematical model uses mathematical language to describe a system by a set of variables and a set of equations that establish relationships between the variables. The actual model is the set of functions that describe the relations between the different variables.

Sets of coupled ordinary differential equations (ODEs), describing a rate of change of a certain variable in the system, can effectively represent chemical reactions. These models offer a quantitative description of the system, allow us to test hypotheses and provide a deeper understanding of the system. Some biological systems display relatively simple dynamic behaviour and will reach a steady-state in a constant environment. Partial differential equations (PDEs) add the ability to represent spatial gradients[83], and stochastic methods make it possible to analyse systems in which the number of molecules is small[84].

With networks of differential equations it is possible to model the temporal and spatial dynamics of biochemical processes in considerable detail. This makes it possible to predict network dynamics under differing conditions by studying the chemical mechanism. It is, however, important to specify the patterns of interaction among the species in the ODE- and PDE-based models in advance. Also, model output is strongly dependent on the values of parameters, usually the initial protein concentrations and rate constants. It is a computationally intensive task to estimate the parameters and it requires substantial data. ODE modelling becomes more and more challenging as the networks get larger, which is why models attempting to capture real biological data are currently limited to a few dozen components[85].

The mathematical framework, MCA (Section 2.3), exists for the quantitative analysis of such a system. Fortunately this framework is not limited to metabolic systems and also allows us to relate high-level systemic properties to low-level components or processes.

2.5.3 Areas of modelling

Within the spectrum of modelling methods currently being applied to cellular biochemistry, kinetic models (example of mathematical models) involving differential equations, bear the closest relationship to underlying biochemical rate laws. One of the most challenging tasks for SB and mathematical biology is certainly the creation of a complete cellular model, which will involve computer simulations of a range of subsystems including metabolism (networks of enzymes and metabolites), signal transduction pathways and gene regulatory networks, in order to analyse the complex connections of all the cellular processes.

Hence, there are many specialised fields each dedicated to solving a part of the puzzle. An example would be that of protein structure prediction, which

is the prediction of the three-dimensional (tertiary) structure of a protein from its amino acid sequence (primary structure). Some scientists view it as one of the most important goals pursued by bioinformatics and theoretical chemistry as protein structure prediction is very important in medicine (i.e. drug design) and biotechnology (i.e. design of novel enzymes).

A great deal of biological modelling has in one way or another, directly or indirectly, the advancement of human health and quality of life as one of its primary goals. Our immune system remains key in this fight, which is why there is a growing number of simulations of the immune system[86,87]. Recently, researchers simulated and tested major portions of the body's immune reaction to the type A influenza virus. Their tests were met with great success and have many implications for the design of treatment and also to plan ahead for future pandemics. This new global model was built from existing, smaller mathematical models, capturing countless interactions between virtual immune cells and viruses[86]. These types of models are used to understand how our immune systems respond to infections, such as the type A influenza virus. Using this model, the researchers performed sensitivity analysis in order to compare the contribution of individual immune cells in the process of fighting the influenza virus. This model can also bring insight into our thinking regarding the working of the immune system[87]. The predicted outcomes of this model simulation is an excellent example of the importance and power of SB.

Ecological modelling

The field of ecology is thought of as a relatively new science as it emerged as a discipline around the second half of the 20th century and then became popular in the 1960s because of a general concern for the environment[88]. Ecological principles have developed steadily and interlinked with other biological disciplines. Of the earliest ecological models were developed by Alfred J. Lotka[89] (1925) and Vito Volterra. Lotka used two first-order, non-linear, differential equations to describe the interactive dynamics of biological systems consisting of two species, a predator and its prey. Volterra independently investigated Lotka's equations in 1926 with statistical analysis of fish catches in the Adriatic[90]. These equations describe the growth of the two species over time.

Ecological modeling is focussed on the mathematical representation of

ecosystems. These models usually focus on simplifying intricate food-webs by breaking them down into their major components, quantifying the components as numbers of organisms, biomass or a concentration of a key nutrient chemical element, like nitrogen or carbon. As a development of theoretical ecology, ecosystem models see to the characterization of the major dynamics of ecosystems in order to gain understanding of these systems as well as the ability to predict their behaviour. Due to extreme complexity, in terms of the number of species and interactions, the system being studied is usually simplified down to a number of components. These components can be, for instance, a species of interest or a broader category, like heterotrophs or autotrophs. Additionally, in biogeochemistry, models might include non-living resources like nutrients being used by the "living" components of the model.

Extensions of ecological modelling

The social ecological model is an interesting part of ecological modelling. Although there are several adaptations of this model, the first and most prominent one was created by Urie Bronfenbrenner in 1977[91]. Ecological Systems Theory, divides factors into four levels, namely macro-, exo-, meso- and micro-, describing influences respectively as either intercultural, community, organizational, and interpersonal or individual. Traditionally only micro, considering individual behaviour, or macro levels, considering cultural or media influences, were distinguished. Bronfenbrenner's perspective included the person, environment as well as the interaction of the two, which is responsible for constant development and evolution of the two components. However, he then realized that instead of the environment directly affecting the person, there were layers between these components, impacting the next level. Bronfenbrenner (1979)[92] believed the individual, organization, community and culture to be nester factors, each one operating within the next larger sphere. Although Bronfenbrenner developed the ecological systems theory, Amos H. Hawley (1950) performed significant research in this field prior to Bronfenbrenner[93].

An interesting application of ecological modeling is modelling the economy on biology, i.e. considering growth, change, death, evolution, survival of the fittest, complex inter-relationships and non-linear relationships. This application to the economy is possible as businesses operate in a complex environment that contains an interlinked set of determinants. This can be

illustrated by the co-evolution of companies as they are influenced by, and influence, banks, suppliers, customers, investors, competitors etc. James Moore suggested that the business environment should be viewed as a business ecosystem, both sustaining and threatening the company in such a way that if the company is not well matched to its environment, it will not survive. Alternatively, if a company has a competitive advantage, it will thrive and possibly come to dominate their industry. These companies are referred to as category killers[94].

Computational neuroscience modelling

Computational neuroscience is defined as the study of brain function in terms of the information processing properties of structures that make up the nervous system[95]. Computational models aim to capture features of these structures on multiple scales, including membrane currents, protein and chemical coupling, network oscillations, columnar and topographic architectures, learning and memory etc. It is then possible to use these models to make predictions and test hypotheses using biological or psychological experiments. Computational neuroscience is an interdisciplinary science linking the diverse fields of neuroscience, cognitive science and psychology with mathematics, physics, electrical engineering and computer science.

Historically, the roots of the field can be traced back to the work of Louis Lapicque, Hodgkin and Huxley, Hubel & Wiesel, and David Marr, to name but a few. The popular integrate-and-fire model of the neuron was created by Lapicque[96] and is used extensively in cellular and neural network studies, including mathematical neuroscience, because of its simplicity[97]. About 40 years later, HH developed the voltage clamp method and created the first biophysical model of the AP[1]. Hubel & Wiesel discovered that neurons in the primary visual cortex have oriented receptive fields and are organized in columns[98]. Also, David Marr described interactions between neurons, particularly how functional groups of neurons interact, store, process, and transmit information[99–101].

Research in computational neuroscience can be roughly divided into several categories. Most computational neuroscientists work closely together with experimentalists, analysing new data and synthesising new models that describe biological phenomena. Intuitively, the simplest category is that of modelling a single neuron. Nonetheless, even single neurons have complex

biophysical characteristics. HH's original model considered only two voltage-sensitive currents, that of the fast-acting Na current and the inward-rectifying potassium current. We now know that there is a wide range of voltage-sensitive currents. The implication of these differing channel dynamics is an important topic of computational neuroscience[102] and there is a large body of literature regarding the interaction of differing currents with neuronal geometric properties[103]. Some models also describe biochemical pathways on a small scale, like synaptic clefts.

This leads to the formation of neuronal systems compromising more than one neuron and the category of axonal development, formation and how the axons are guided to their proper position. From molecular biology we know that the nervous system releases chemical signals, such as growth factors and hormones, which modulate and influence growth and development of neuronal connections. Although studies regarding the formation and patterning of synaptic connections are yet to deliver promising results, there is one hypothesis that has gained some attention - the minimal wiring hypothesis, postulating that axonal and dendritic formation minimises resource allocation while still maintaining maximal information storage[104].

Considering sensory processing, early theoretical models are credited to Horace Barlow who postulated that early sensory systems, somewhat similar to the minimal wiring hypothesis, efficiently encoded information by using the minimal number of spikes[105]. This hypothesis has since been supported both experimentally and computationally. Currently, research in this field is divided into biophysical modelling of subsystems and the more theoretical modelling of perception. Current models of perception suggests that the brain processes and functions by integrating different sensory information and utilizing some form of Bayesian inference[†] in order to generate our perception of the physical world.

Earlier models of memory are primarily based on the postulates of Hebbian learning, introduced by Donald Hebb in 1949[106], which states that persistent stimulation of the postsynaptic cell by the presynaptic cell will increase synaptic efficacy. In biological systems the associative rather that content-addressable style of memory is used and biological models have been developed to describe these properties[107]. These attempts are, however, focussed on medium- and long-term memory formation, as localised in the hippocampus.

[†]Bayesian inference is statistical inference that uses observations to update or infer the probability that an hypothesis may be true.

Working memory models rely on network-oscillation and persistent-activity theories and have been built to capture features of the prefrontal cortex in context-related memory[108]. Neurophysiological memory is constantly maintained and changed, posing a problem for modelling as unstable synapses are easy to train but prone to stochastic disruption. On the other hand, stable synapses forget less easily, but they are also harder to unite. A recent computational hypothesis, involving cascades of plasticity[109], allow synapses to function at multiple time scales. Stereochemically detailed models of the acetylcholine receptor-based synapse with the Monte Carlo method have been built, working on a microsecond time scale[110]. In the next few years it is likely that computational tools will greatly contribute to our understanding of how synapses function and change in relation to external stimulus. In fact, Kotaleski and Blackwell[6] have reported some of these recent advances by using systems biology approaches in modelling the molecular mechanisms of synaptic plasticity.

There are many software packages that allow rapid and systematic *in silico* modelling of realistic neurons. Various software packages and simulation tools are used, such as Emergent[111] and Genesis[112] for general neuronal simulation, NEST[113] and NEURON[114] for simulation of large neuronal systems, Neuroconstruct for the development of biologically realistic 3D networks[115], neuroscience related Python tools such as pyNN[116] and Neurospaces[117], a simulation system that uses industry-related software engineering principles. Blue Brain, a project founded by Henry Markram, aims to construct a biophysically detailed simulation of a cortical column on the Blue Gene supercomputer[118].

2.6 Neuronal signalling and modelling of the action potential

When a combination of graded potentials from neighbouring neurons push a neuron membrane potential above the threshold (-55mV), an AP is triggered at the triggering zone on the axon hillock. This part of the neuron has a lower threshold due to an abundance of sodium channels making it more sensitive to changes in membrane potential. The AP is then conducted along the axon to the axon terminals where the signal is passed to effectors or other neurons.

Signal conduction in the axon occurs as a result of its membrane properties,

in particular sodium and potassium membrane channels. The resting membrane potential of -60 mV (some cells have a slightly more negative resting potential) is largely due to the semi-permeable cell membrane which traps larger anions in the intracellular fluid (ICF), causing the inside of the cell to be negatively charged relative to the outside. Sodium is concentrated in the extracellular fluid (ECF) while potassium is concentrated in the ICF. Thus, if sodium and potassium channels were to open, sodium will diffuse into the cell and potassium out of the cell. When an AP is triggered by a stimulus, there is a depolarisation of the membrane which causes the voltage-gated sodium channels to open. The influx of sodium causes further depolarisation. When the membrane potential reaches 0 mV, the sodium influx is no longer caused by electrical potential (attraction of opposite charges), but because of a higher sodium concentration in the ECF. The still rising membrane potential, peaking at +30 mV, now causes the sodium channels to close, while the potassium channels are slowly opened. The repolarisation phase of the AP is characterised by an efflux of potassium ions down its electrochemical gradient, decreasing the membrane potential causing hyperpolarisation due to slow-closing potassium channels. Permeability of the membrane is now returned to its resting state while the extra efflux of potassium moves back into the cell, repolarising the membrane potential to the resting state of $-60\,\text{mV}$. Lastly, ionic distributions are quickly restored (by sodium-potassium anti-porters) to the balance observed in the resting state.

In the early 1950's, HH were at the forefront of experiments that led to the characterisation of this signalling mechanism. Intuitively, they began their research using a single neuron. Since their research, various experiments on neurons have led to even more detailed characterisation, including that of neural networks. Advances in neurobiology therefore led to the creation of computer models which enabled researchers to explain neuronal behaviour and make further predictions. Neuroscience is now an interdisciplinary science and includes many different approaches to study various aspects of the nervous system. The increasing use of computer models in these studies has been and continues to be of immeasurable value, also to make predictions. The earliest model to describe neuron behaviour was the HH-model which described the properties of a single neuron with great accuracy. In the rest of this section, we will first present the HH-model and its formal description, then focus on analyses and modifications to the model, ending with motivating our choice of model to use in this analysis.

2.6.1 The Hodgkin-Huxley model

The mathematical model constructed by HH explains the AP and its propagation along the axon of a neuronal cell. This model is an example of a kinetic model which describes a cellular function emerging from the interaction between molecular components, using nonlinear differential equations. Being one of the first numerical simulations in biology to be published, the construction of this model is regarded by some as the beginning of computational SB[79]. The following part will focus on how HH built this model, specifically on their experimental design, parameter estimation, the formal equations and the model outcome.

Model construction and description

HH performed a series of experiments that allowed them to measure the time and voltage dependence of the sodium and potassium conductances. In their experiments they used the squid giant axon, which has a diameter of half a millimeter, making it suitable for experimental research. They employed a few experimental methods in order to obtain the conductances. These methods include a space clamp, where a long, thin electrode is inserted in the axon which keeps the membrane potential equal along the whole axon. This allowed them to view the axon as a small patch of membrane considering that a supra threshold stimulus would then result in the whole membrane participating in one membrane AP. Crucial to this method is the voltage clamp, consisting of two electrodes. The one electrode applies a constant current in order to keep the membrane potential clamped to a specified value. The second measures the change in membrane potential and modulates the applied current in order to keep it clamped at that the specified value. They were thus able to measure change in ion conductances as the ion concentrations in the bulk fluid changed upon depolarisation of the clamped axon[1].

With these measurements, they determined the properties of the excitable axonal membrane and did so with remarkable accuracy. From their research, they constructed a set of four differential equations and a few supporting functions, which will now be explained. The main equation (Eq. 2.5) describes the membrane as a non-linear electric circuit:

$$I_m(t) = C_m \frac{dV}{dt} + \bar{G}_K n(t)^4 \left[E_K - V(t)\right] + \bar{G}_{Na} m(t)^3 h(t) \left[E_{Na} - V(t)\right] + \bar{G}_{leak} \left[E_{leak} - V(t)\right] - I_{ext}(t). \quad (2.5)$$

Eqs 2.6-2.8 describe the ion channels

$$\frac{dn}{dt} = f_n V(t) \left[1 - n(t)\right] - q_n V(t) n(t), \quad (2.6)$$

$$\frac{dm}{dt} = f_m V(t) \left[1 - m(t)\right] - q_m V(t) m(t), \quad (2.7)$$

$$\frac{dh}{dt} = f_h V(t) \left[1 - h(t)\right] - q_h V(t) h(t). \quad (2.8)$$

The activity of the respective channel is dependent on the state of the channel, which is described by gating particles - for potassium (n) and sodium (m - activating and h - inactivating) which are functions of the membrane potential.

The state of the each channel is determined by two rate constants (voltage dependent functions), f and q, which can be compared respectively to the phosphorylation (via kinases) and dephosphorilation (via phosphatases) of an enzyme. Eqs 2.9-2.14 describe two rate constants for each of the respective gating particles

$$f_n = 0.01(V + 10)/(\exp\frac{V + 10}{10} - 1), \quad (2.9)$$

$$q_n = 0.125 \exp(V/80), \quad (2.10)$$

$$f_m = 0.1(V + 25)/(\exp\frac{V + 25}{10} - 1), \quad (2.11)$$

$$q_m = 4 \exp(V/18), \quad (2.12)$$

$$f_h = 0.07 \exp(V/20), \quad (2.13)$$

$$q_h = 1/(\exp\frac{V + 30}{10} + 1). \quad (2.14)$$

For reference, the first term of each of the gating particle equations (Eqs 2.6-2.8) will be referred to as rate constants α_n, α_m and α_h respectively, while the second term of each equation will be referred to as rate constants β_n, β_m and β_h respectively.

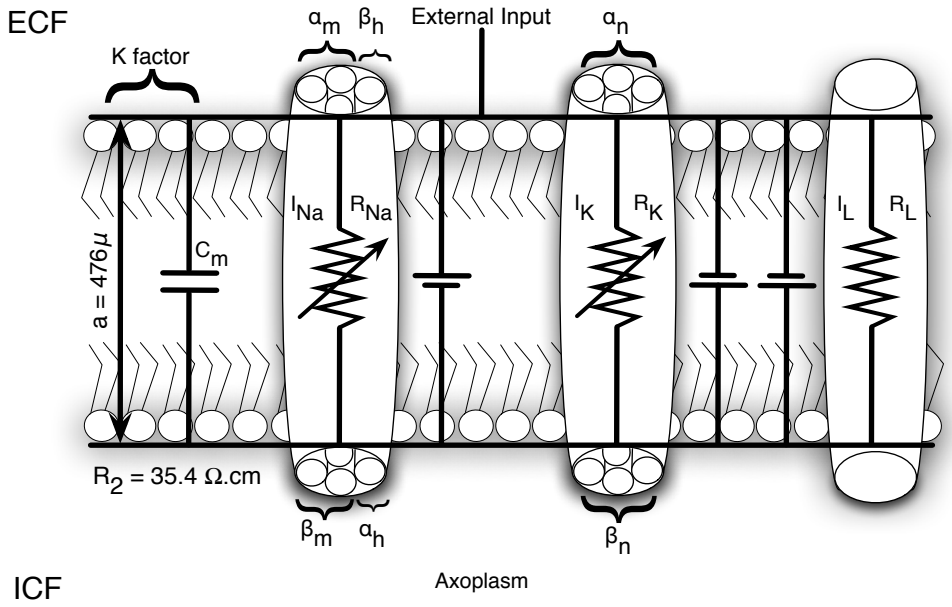

Figure 2.2: The HH circuit diagram superimposed on a biological axon membrane.

Rate constants α and β describe the "movement" of the gating particles from one side of the membrane to the other; for instance α_m, β_h and α_n would drive the gating particles (m, h and n) to the intracellular (ICF) side. When the gating particles are located at the cytosolic side (ICF - Fig. 2.2) of the membrane, they are functional, and at the extracellular side (ECF - Fig. 2.2), they are inactive.

When they constructed the model, HH did not know of the existence of membrane channels that allow the flow of ions across the membrane, effectively bringing about the AP. Interestingly, their equations of the mechanistic description of the sodium and potassium channel gating particles coincide with the number of respective biological channel subunits (see Eqs 2.20 and 2.21).

The HH-model is a biophysical model and as such an electrical equivalent can be constructed to describe the membrane and all its properties. The resulting circuit is shown in Fig. 2.2.

A capacitor (C_m) accounts for the membrane's ability to store charge. Resistors describe the ion channels that are embedded in the membrane and the batteries represent the electrochemical forces that influence the current due to imbalanced ion concentrations on the inside (ICF) and outside (ECF)

of the cell (Fig. 2.2).

The total membrane current is thus the sum of the ionic currents and the capacitive current:

$$I_m = I_{ionic} + C_m \frac{dV}{dt}. \tag{2.15}$$

The model considers three ionic currents: sodium and potassium, which are voltage-gated and time dependent, and a leak conductance that is independent of the membrane potential (Fig. 2.2)

$$I_{ionic} = I_{Na} + I_K + I_{leak}. \tag{2.16}$$

Both types of current are linearly dependent on the membrane potential as described by Ohm's law $I = {}^{V}/_{R}$. Considering the electrical circuit is based on biological components, resistance is rather referred to as conductance $G = {}^{1}/_{R}$. The potential the ions experience is expressed by two terms: the driving potential $V(t)$ and the reversal (equilibrium) potential E_k at which the net current of that ion across the membrane is zero (the ionic current due to the electric field cancels the current due to the concentration differences across the membrane). E_k is given by the Nernst equation. The ionic current of a species k is given by

$$I_{ionic} = G_k(E_k - V). \tag{2.17}$$

Since I_{ionic} is the sum of individual currents, it leads to

$$I_{ionic} = G_K(E_K - V) + G_{Na}(E_{Na} - V) + G_{leak}(E_{leak} - V). \tag{2.18}$$

The ion channels represented by these ionic currents are gated by a selectivity filter (a part of the ion channel where protein loops reach into the opening and narrow it considerably). This filter controls the flow of ions through the channel. Individual loops (or gates) can be in either a permissive or non-permissive state. Only when all gates of an individual channel are permissive, the channel is open and a current can pass through. HH defined the probability for a gate to be found in its permissive state to depend on the membrane potential, therefore incorporating the voltage dependent conductance. Conductance is proportional to the number of open channels which are in turn proportional to the number of permissive gates. The conductance of channels for ion type k is therefore proportional to the product

of probabilities p_i of gate type i

$$G_k = \bar{G}_k \cdot \prod_i p_i \tag{2.19}$$

bearing the maximal possible conductance. This leads to specific equations for potassium and sodium conductance

$$G_K = \bar{G}_K p_n^4 = \bar{G}_K n^4, \tag{2.20}$$

$$G_{Na} = \bar{G}_{Na} p_m^3 p_h = \bar{G}_{Na} m^3 h \tag{2.21}$$

and finally

$$\begin{aligned} I_m(t) = C_m \frac{dV}{dt} + \bar{G}_K n(t)^4 \left[E_K - V(t)\right] + \bar{G}_{Na} m(t)^3 h(t) \left[E_{Na} - V(t)\right] \\ + \bar{G}_{leak} \left[E_{leak} - V(t)\right]. \end{aligned} \tag{2.22}$$

In the case of the propagated AP, Eq. 2.5 can be related to a PDE. Eqs 2.6-2.8 remain unchanged. The PDE describing the HH-model AP propagation requires the incorporation of a factor (K) consisting of the radius of the axon a, the specific resistance of the axoplasm R_2 and the capacity C_m per unit area of membrane[1] (refer to Fig. 2.2). This leads to the following relation of the membrane current density

$$I = \frac{a}{2R_2} \cdot \frac{\partial^2 V}{\partial x^2}, \tag{2.23}$$

with

$$K = \frac{a}{2R_2 C_m} \tag{2.24}$$

and thus

$$\begin{aligned} K \frac{\partial^2 V}{\partial x^2} + \frac{\partial V}{\partial t} = \frac{1}{C_m} \big\{ & -\bar{G}_K n(x,t)^4 \left[E_K - V(x,t)\right] \\ & -\bar{G}_{Na} m(x,t)^3 h(x,t) \left[E_{Na} - V(x,t)\right] \\ & -\bar{G}_{leak} \left[E_{leak} - V(x,t)\right] + I_{ext}(x,t) \big\}. \end{aligned} \tag{2.25}$$

Eq. 2.5 (ODE) is therefore transformed into Eq. 2.25 (PDE). The HH-model was reconstructed using Mathematica from the original publication[1]. Apart from an accurate description of the firing properties of the AP, their model accurately describes the AP shape as well as the propagation velocity of the travelling AP wave. The propagation speed as described by the model corresponds well with experimental values and thus also served as model validation.

Historical perspective

The HH-model was created 58 years ago, hence many extensions of neuronal models have been created since. Over the last half a century, different analyses have been done on different versions of the HH-model (original or modified) and in different systems (single as well as multiple neuron), both experimental and model simulation, and in neuronal tissue from differing animals. As the original HH-model describes the characteristics of a single neuron, we will keep our focus on single neuron studies. As there are a multitude of studies on neuronal models and the HH-model especially, the studies that we have found have been divided into categories of type of study, as indicated below.

Some of the models more directly related to the HH-model include the Fitzhugh-Nagumo[119,120], Morris-Lecar[121] and Hindmarsh-Rose[122] models, that consist of reduced equations. Many models, including the HH-model[123,124], have been extended to include stochasticity in their description. These single neuron models (with stochastic behaviour incorporated) are used in numerical studies[125], studies to determine the effect of toxins/inhibitors[126,127], studies to determine the workings of a specific neuronal mechanism[128] and in studies that compare, for instance, a specific behaviour of two differing types of models[128,129]. There are also a few models, mostly based on the HH-model, that describe the characteristics of the AP, but with a mathematically reduced set of equations. These are used in bifurcation studies[130–132], studies to determine a specific mechanism[133] as well as in studies using singular perturbation theory[130].

In the following part, studies that used other neuron types in their analyses will be mentioned first, followed by studies that used the squid axon with modified equations, followed by studies that used the squid axon with the original model parameters.

Many studies utilized other neuron types and hence models with modified

parameters and/or equations from the original HH-model. Consisting of experimental and/or simulation studies, their analysis type includes the mechanism responsible for specific behaviour, for instance, how efficiently sodium entry is coupled to depolarisation[134], the effect of high sodium concentration on AP characteristics[135], the mechanisms that mediate depolarization-induced spike activity in pancreatic cells[136] and the influence of ion dynamics on excitability and seizures[132] among others[137–139]; comparing the ionic working of the HH-model to that of a mammalian retinal ganglion cell model[140]; toxin/inhibitor studies to determine the effects of local anaesthetics in single, myelinated frog sciatic nerve axons[141], to determine the binding characteristics of a toxin to the membrane of rabbit cervical vagus nerve[142]; and using sensitivity analysis to examine the contribution that neuronal response dynamics have on functional properties of the system[139,143].

Models of the single squid axon with modified parameters/equations have been studied in terms of bifurcation analysis[144]; sensitivity analysis of the strength-duration relationship to changes in sodium channel parameters[145]; the use of toxins/inhibitors to determine the effect on AP firing frequency and possible targets in disorders in neuropsychiatry or cardiology[146], or the effect on AP characteristics such as height, propagation speed and the effect on channel dynamics[147]; determining the kinetics of ion channels to determine whether channel densities and transition rates are optimized for signal sensitivity and propagation speed[148], or a reparameterised HH-model to compare more accurately to the experimental AP velocity and also optimisation of channel density[149] and determining the metabolic cost of the AP and its propagation, comparing the original and a reparameterised model so as to identify a possible easily evolvable parameter to lead to more effective use of energy[150].

And finally, the following analyses have been done on a single squid axon with original parameters:

- numerical examination of the effect on neuronal spiking by applying the weak periodic perturbation to the HH ion channels to influence chaotic behaviour[151] and
- analyzing the non-linear dynamics of the model and present some modifications in the equations[152]
- bifurcation analyses[153–158]

- mechanistic analysis to determine the neuron response when stimulated by a sequence of high-frequency conductance pulses[159] and
- exploring the controllability of switching between spike generation and spike annihilation[158]
- comparing macroscopic membrane currents of the HH equations to discrete microscopic stochastic ion channels populations[128]
- exploring the effect of toxin TTX on squid axon membrane (sodium) channels in terms of kinetic binding properties and how it affects the AP properties like amplitude, propagation velocity and frequency[160–163]
- metabolic energy cost determination to investigate whether the inactivation properties of sodium channels show evidence of being optimised in terms of energy expenditure in the propagation of APs[164].

Since our study involves MCA and hence the effect of component perturbation, as opposed to sensitivity analysis for instance, the HH studies can be narrowed further to perturbations of components. Experimentally, there have been a number of toxin/inhibitor studies performed on the squid giant axon as well as other neurons, as mentioned above. Of those performed on the squid axon, a study by Culquhoun and Ritchie (1972)[162] stands out as they used the sodium channel inhibitor, TTX, to determine its effect on properties of the AP. As TTX exerts its inhibiting effect on the sodium current solely though the sodium conductance, which can be seen as the total number of functioning sodium channels, it functions as a perturbation of the sodium channel. Considering model simulation, Shapiro and Lenherr (1972)[165] studied the effect of perturbations in sodium and potassium channel conductance and activation kinetics on the firing frequency of the AP. Although these theoretical studies report both the qualitative and quantitative effect of a single component perturbation on some AP characteristics, they do not account for all the components of the system and thus cannot use summation theorems in their analysis. To the best of our knowledge, MCA has not been performed on a neuronal model making our analysis of the HH-model novel.

Why HH when other models exist

In its mathematical description, the HH-model distinguishes between biological components. This allows us, through the use of MCA, to determine the

amount of control that each component has on the emergent behaviour of the system. As mentioned above, since the HH-model is an older and relatively simple model, it comes as no surprise that numerous, much newer models, have subsequently been constructed. These models have either a more accurate description of the modelled behaviour or incorporate more complex phenomena, or a combination of both. Where the HH-model complements our method of analysis, we encountered databases such as ModelDB (http://senselab.med.yale.edu/)[166], which contain models describing the behaviour of various types of neurons, both single neurons and networks, which do not. Our criteria "exclude" neuronal networks and mathematically complex descriptions because our analysis methodology requires a model that mathematically distinguishes biological components (see Section 2.3). There are, however, a few single neuron models that compare to and have been largely deduced from the HH-model, which will briefly be discussed.

In 1961 FitzHugh and Nagumo constructed a simplified version of the HH-model by isolating the mathematical properties of excitation and propagation from the electrochemical properties of sodium and potassium ion flow[119]. Their model, however, was not clearly derived from biology, making the biological components mathematically indistinguishable[120]. A few years later, in 1981, Morris and Lecar combined the HH and FitzHugh-Nagumo models into a voltage-gated Ca channel model with a delayed-rectifier potassium channel[121]. Their model contained no sodium channel description and no distinguishable gating characteristics like the HH-model. Still later, Hindmarsh and Rose (1984) constructed a model by distinguishing between fast and slow ion channels: sodium and potassium are both included in the fast channels which resulted in a lack of mathematical distinction between the sodium and potassium currents[122].

Although it might be possible to analyse abovementioned, more complex models, our work serves as an illustration of the type of analysis that can be done on neuronal systems. Not only does the distinction of biological components in the HH-model allow us to relate to experimental perturbations of components, we also saw it appropriate to illustrate our analysis approach on one of the most well-known models in neurology.

2.7 Channelopathies

As mentioned in the beginning of this chapter, our nervous system provides crucial support to our everyday life. It does so via constant neuronal signalling back and forth between organ systems. That is why the correct functioning of the neurons that transfer these signals, is of great importance. Mutations in the components of the neuron, particularly the ion channels, can, however, occur. This can lead to changes in signalling, which in turn, can lead to pathological neuronal behaviour, such as epilepsy. These changes in ion channels that result in such pathological behaviour, are known as channelopathies[2,167]. Many mutations behind pathological behaviour have been characterised. In general, if a mutation leads to an increase in AP firing frequency (increase in neuronal hyper-excitability), it will result in epileptic behaviour. In this section, some of the characterised mechanisms behind a specific type of epilepsy will be mentioned, which will also serve to pave the way for a more detailed discussion (in Chapter 4) regarding how these mechanisms compare to our analysis results.

Since the discovery of the first human epilepsy-associated ion channel gene mutation more than a decade ago, mutations in at least 25 different genes implicated in channel structure have been discovered. Some of these mutations are situated in the voltage-gated sodium[2,3,168,169] and potassium channels[170–173]. Significant advances have been made in our understanding of the molecular deficits caused by these mutations. The link between molecular deficit and clinical phenotype, however, still seems to elude us[174]. Reid et al. (2009) compiled data describing genes and their associated epilepsy syndrome as well as semi-quantitative estimates of associating the epileptic phenotype to the gene[174]. The KCNQ2/3 and SCN2A gene mutations will briefly be discussed below.

Benign familial neonatal infantile syndrome (BFNIS) has been shown to cause convulsions in newborns[170–173]. A mutation implicated in BFNIS is located in the genes coding for the muscarinic-regulated potassium current (M current, not to be confused with the sodium gating particle) that activates and deactivates potassium conductance[173]. This current was first described in peripheral neurons[175] and subsequently in the CNS[176] and is a widespread regulator of neuronal excitability. According to Rundfeldt and Netzer (2000)[177] and Main et al. (2000)[178], potassium conductance in the neuron is mediated by KCNQ2/KCNQ3 potassium channels. The mediation

of potassium conductance is necessary in order to limit repetitive firing[179–181]. A specific mutation (R214W) in the voltage-sensing S4 domain of KCNQ2 subunits of this channel, causes an arginine to tryptophan substitution[182]. This results in a moderate loss of function (reduction in potassium current) which decreases the AP threshold[183] causing a decrease in seizure threshold leading to hyperexcitability. This mechanism leads to BFNIS.

Considering the sodium channel, two mutations (among others), in the α unit of a sodium channel (SCN2A), L1563V and L1330F, have also been linked to BFNIS[168,169]. Scalmani et al (2006)[184] reported differing mechanisms for four of these mutations. Experimentally, it was found that the L1563V mutation causes a negative shift of the curve of voltage dependence of activation, thus enhancing activation. The L1330F mutation, however, caused a positive shift of the voltage dependence of the inactivation curve, reducing inactivation. Even though there is heterogeneity in the way the ion channel properties are modified, it is thought that all SCN2A mutations result in a gain in channel function and an increased sub-threshold sodium current (reducing firing threshold), leading to neuronal hyper-excitability (increased AP firing frequency)[184].

The detail of our model predictions corresponding with the experimental work, as compiled by Reid et al.[174], will be discussed in Chapter 4.

Chapter 3

Results*

3.1 Introduction

Axons carry information across the nervous system in the form of APs. The early work by HH has been instrumental for our mechanistic and quantitative understanding of the AP[1]. In their experimental work on the squid giant-axon they determined the time and voltage dependence of the Na and K conductances, via measurements of ion concentration changes in the bulk fluid. As a result, in their model (HH-model) a single Na and K conductance is described, but it is representative for the complex kinetic characteristics found in the neuronal axon. The HH-model uses both ODEs and PDEs to describe various high-level behaviour of the AP and it predicts propagation properties of the AP with great accuracy despite its simplistic nature.

The combination of experiment, theory and modelling used by HH is a good example of a SB study. The authors fitted kinetic parameters to experimental data of the systems processes (ion-channels), to predict systems properties (propagation of AP). Despite the importance of the HH-model and it having been analysed in many studies, it is not known to what extent the different processes in the system contribute to the system's behaviour. Such an analysis, which would be typical for a SB study, has not been done for the HH-model. A number of reasons for the limited overlap between SB and computational neuroscience studies have been indicated in De Schutter (2008)[5]. We here aim at narrowing that gap by using a SB method (MCA) to analyse one of the best studied models in neuroscience and test whether this method leads to

*The work presented in this chapter is intended for publication, and will therefore have some overlap with Chapters 2 and 4.

additional insight into the system. In addition we show how control analysis can be applied to wave propagation (i.e. propagation of the AP).

MCA, independently formulated by Kacser and Burns (1973)[8] and Heinrich and Rapoport (1974)[9] is a rigorous quantitative framework that defines control of the reaction steps within a biological network on system properties of that network, e.g. the control of flux in a metabolic pathway by the enzymes in the pathway. The framework has mostly been applied to steady-state (non-transient) systems, but the theory and methods have been extended to include dynamic systems[75]. The framework should not be confused with a more traditional sensitivity analysis, where all parameters are perturbed. In MCA not the parameters of the system, but the processes of the system are perturbed. This leads to the formulation of summation and connectivity theorems (non-existent in sensitivity analysis) in which relations between the control coefficients (system properties) and elasticity coefficients (processes properties) are expressed. MCA has been extended to dynamic systems[69,73,74] and summation theorems have been derived for such systems[75]. It has, however, not been possible to derive connectivity theorems for dynamic systems.

Since this study is the first to report on MCA for a neuronal system, we start with explaining how such an analysis can be performed on characteristics of the AP and its propagation, using the HH-model. The summation theorems for the systems properties are given and the analysis results are compared to experimental perturbations (inhibitor studies) of some of the systems processes, followed by a description of the mechanistic working of the system upon a process perturbation.

3.2 Results

3.2.1 MCA of the AP properties in the HH-model

MCA is usually applied to steady-state systems such as metabolic pathways, for which the contribution of the enzymes in the pathway to the control of the steady-state flux and metabolite concentrations can be quantified. In addition, MCA has also been applied to the frequency and amplitude (i.e. stationary behaviour) of oscillatory systems and most recently to transient behaviour, for instance in signal transduction pathways. For our MCA of the AP, we start with the MCA analysis of time invariant system observables, e.g. AP peak and

propagation speed, and link this to experimental perturbations of the system. We will then show the analysis of the model's state variables during an AP and end with an analysis of the feedback loop contribution to the progression control of a process on a system variable in an attempt to illustrate how a perturbation in a system process affects the system.

In the HH-model the total membrane current is split into four processes: Na, K and Leak currents and an external input (stimulus). The currents through the ion channels are dependent on their conductivity ($\bar{G}_K$, $\bar{G}_{Na}$, $\bar{G}_{Leak}$), which can be interpreted as the total concentration of a respective channel that is present in the axon membrane. In addition, the activity of the channels is dependent on their "state", which is defined by gating particles (n, m and h, for K channel activation, Na channel activation and Na channel inhibition respectively).

The state of the each channel is determined by two rate constants (voltage dependent functions), f and q, which can be compared respectively to the phosphorylation (via kinases) and dephosphorilation (via phosphatases) of an enzyme. However, we viewed the rate constants and the respective parts of the gating particle equations as similar and termed them α and β rate constants although they refer to a function (See Section 3.4.3).

The gating particles can be located at the cytosolic side of the membrane (where they are functional) or at the extracellular side (where they are inactive). Thus, for each of the gating particles an α and β rate constant describes the movement of the gating particles from the extracellular to the cytosolic side of the membrane (α_n, α_m, β_h) and vice versa (β_n, β_m, α_h). Thus, an increase in $\bar{G}_{Na}$, α_m or α_h, which respectively leads to an increase in the Na channels, an increase in the Na activating and a decrease in the Na inhibitory particles, leads to an increase in the current through the Na channel.

These ten processes (three conductivities, six rate constants for transport of gating particles and the stimulus) define all the catalytic steps in the HH-model and are used for the MCA of this model. As an illustration, in Fig. 3.1 the effect of a 10% decrease of the Na conductivity is shown to decrease the AP amplitude and the firing frequency. With MCA such an effect can be quantified with a control coefficient as the percentage change in AP or firing frequency upon a 1% change in channel activity.

Although the HH-model was originally formulated as a PDE it is usually simulated in terms of ODEs. Under assumption of a constant form of the AP, the PDE that describes the propagating AP can be translated (using the

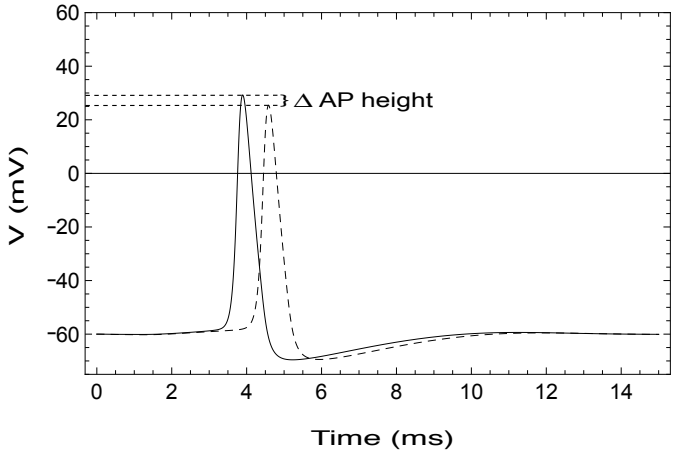

(a)

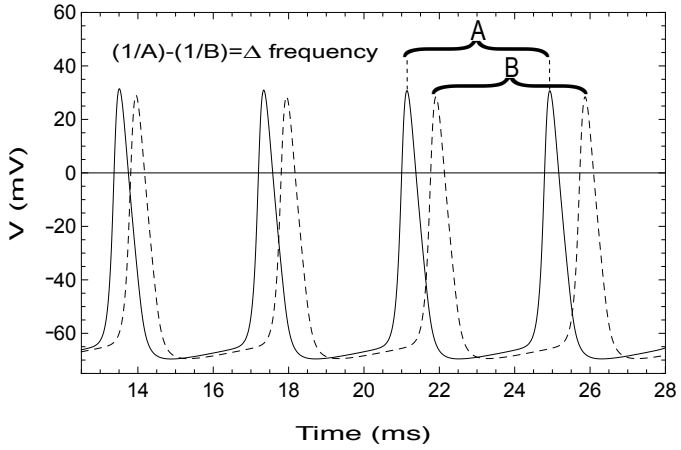

(b)

Figure 3.1: Simulation result for the HH-model after a 10 mV stimulus for 4 ms (a) and a continuous 25 mV stimulus (b). The solid line shows the simulation result for the original model parameters, while the dotted line indicates the result after a 10% perturbation of the Na channel. In the graph it is indicated how the control coefficients on AP height and frequency were calculated. This large a perturbation is intended for the graphical illustration only and small perturbations were used for the calculation of control coefficients. For more detail on the MCA calculations, see Section 3.4.5.

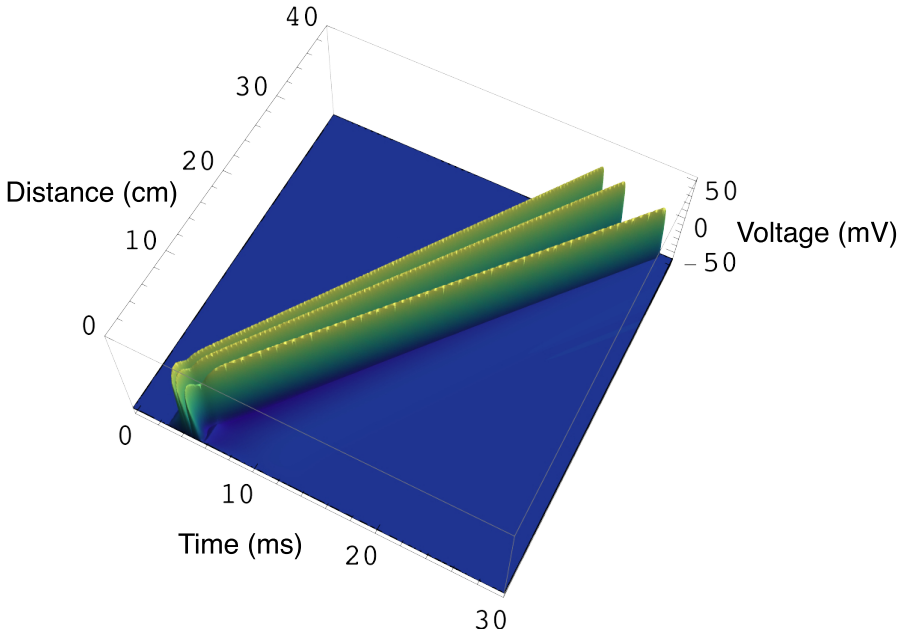

Figure 3.2: Propagation of the AP and the effect of Na channel inhibition in the PDE formulation of the HH-model. After an initial stimulus (15 mV for 3 ms) an AP is generated (membrane potential on z-axis) which propagates with time (x-axis) along the axon (distance on y-axis). The simulation describes the system at 18.5°C resulting in a propagation speed of 19.55 m/s (top graph). The effect of a 20% (middle graph) and 40% (lower graph) inhibition of the Na channel on the propagation of the AP is shown.

cable equation) into a set of ODEs. We have here simulated the HH-model in its original PDE form for the analysis of the propagation speed of the AP. Similarly as for the AP peak and the firing frequency we can analyse the effect of a perturbation on the propagation speed of the AP. In Fig. 3.2 we show the simulation result for the PDE formulation of the HH-model, and the effect of a 20% and 40% blocking of the Na channel. For its MCA we used the PDE version of the HH-model for the analysis of the propagation speed and the ODE version for the analysis of the other system characteristics.

The control coefficients for the threshold, AP peak, propagation speed and firing frequency are listed in Table 3.1. The analysis shows that perturbation of any process leading to an increase in Na current (i.e. $\bar{G}_{Na}$, α_m, α_h) amplifies the AP (i.e. lowers the threshold, increases the AP peak, the propagation speed and firing frequency). The opposite holds for the K channel. The control coefficients do not only describe the qualitative behaviour but quantify the effect of the perturbation. Thus, whereas the Na channels amplify the AP

Table 3.1: Control coefficients of the system processes on the threshold, AP peak, AP propagation speed and frequency. The process K-factor is included only in the propagation speed as the PDE model was used for this simulation. Control is distributed across the system processes such that the control coefficients sum up to either 0 or 1.

Nr	Process	Threshold	AP peak	Propagation speed	Firing Frequency
1	K-factor	-	-	0.500	-
2	$\bar{G}_{Na}$	-2.201	0.915	0.324	0.492
3	$\bar{G}_{K}$	2.401	-0.650	-0.056	-0.623
4	$\bar{G}_{Leak}$	0.055	-0.160	-0.035	-0.022
5	Ext. input	-0.731	0.030	0.000	0.304
6	α_n	7.648	-1.696	-0.145	-1.554
7	β_n	-6.999	1.204	0.092	2.003
8	α_m	-6.078	1.726	0.586	1.491
9	β_m	5.767	-1.265	-0.158	-1.333
10	α_h	-0.670	0.490	0.131	0.291
11	β_h	0.809	-0.594	-0.239	-0.048
$\sum$		0.001	0.000	1.000	1.001

signal, it can be seen from the table that the α and β rate constants that effect the state of the channel (a function of the gating particles) have higher control coefficients than the concentration of the channel ($\bar{G}_{Na}$). Specifically, rate constants for the m and n gating particles have high control, which reflects the third and fourth order of these particles in the model description of the total current (see Eq. 3.6 in Section 3.4.3).

The last and most distinctive aspect of the control coefficients as defined in MCA lies in their inter-relation; from the summation theorems for the control coefficients it can be seen that the control on the systems properties are necessarily distributed over the system. There is not a single "rate-limiting step" or "master-controller", but the control is distributed over the system, such that the control coefficients sum up to either 0 or 1. The summation theorems for the AP peak, threshold, firing frequency and propagation speed can be summarised as:

$$\sum_{i=1}^{10} C_i^{\text{AP height}} = 0, \tag{3.1}$$

$$\sum_{i=1}^{10} C_i^{\text{threshold}} = 0, \tag{3.2}$$

$$\sum_{i=1}^{10} C_i^{\text{firing frequency}} = 1, \tag{3.3}$$

$$\sum_{i=1}^{11} C_i^{\text{propagation speed}} = 1. \tag{3.4}$$

These summation theorems distinguish MCA from a sensitivity analysis. The summation theorems show that when all system processes are perturbed equally, this will leave the AP height and threshold unchanged (i.e. sum up to 0, comparable to amount/concentration related quantities), while the firing frequency will change in proportion to the perturbation, i.e. a 10% change in all processes will lead to a 10% increase in firing frequency (i.e. sum up to 1, comparable to rate- or flux-related quantities). This is because a simultaneous perturbation of all the processes, say an increase, would have the effect of speeding up or scaling the whole simulation which would change a property that has a time component in its description accordingly. The summation theorems for oscillatory frequency and amplitude have already been derived for other systems and our summation results correspond with earlier MCA studies on frequency and amplitude (AP height)[70,73,185–187].

The difference between the analysis methods lies in the definition of system process, which in MCA terms would be a catalytic step (for instance an enzyme activity), while in a sensitivity analysis all model parameters are perturbed. This is important as it makes MCA more than a tool for model analysis but gives a direct link to experimentation, where often systems processes are perturbed, for instance via inhibitor titration experiments.

3.2.2 Experimental MCA; inhibitor titration of Na channel

Certain neurotoxins, such as tetrodotoxin (TTX), block the Na channels of the axon, thereby preventing it from firing. Takata et al.[188] and Hille[189] have

suggested that the m and h parameters are not affected by TTX and that the effect of the toxin is solely on the $\bar{G}_{Na}$. Inhibitor titrations have been published for the isolated Na channels[161] where the proportion of free channels (P_f) as a function of the TTX concentration was determined. In another set of experiments, similar TTX titrations were made and the effect on the AP peak and propagation were measured[162].

From these data sets the percentage inhibition of the Na channel and its effect on AP peak and propagation can be calculated. To obtain the physiological relevant conditions one needs to estimate the effects of perturbations at zero inhibitor concentrations (i.e. $\lim_{TTX\to 0}$). The effect of TTX on system property Y, via its inhibition of the Na channel can be described by

$$R^Y_{TTX} = \epsilon^{P_f}_{TTX} \cdot C^Y_{P_f}. \tag{3.5}$$

This equation describes the percentage change in property Y upon a 1% change in TTX concentration (R^Y_{TTX}), as the multiplication of the inhibitory effect of TTX on the Na channel ($\epsilon^{P_f}_{TTX}$) and the control of Y by the Na channel ($C^Y_{P_f}$). From the data sets plotted in Figs 3.3a, 3.3b and 3.3c respectively the unscaled parameter elasticity $\partial(P_f)/\partial(TTX)$, and response coefficients $\partial(prop.speed)/\partial(TTX)$ and $\partial(APpeak)/\partial(TTX)$ can be obtained at zero TTX. From these the control coefficient of the Na channel on the respective properties can be calculated by taking the ratio of the response and elasticity coefficients (Eq. 3.5). In this way we calculated the control coefficient for the Na channel on the AP peak and AP propagation speed to be 0.1 for both characteristics. This control coefficient is much lower than the coefficient that was obtained from the HH-model analysis (i.e. 0.9 and 0.3 respectively for the control of AP peak and AP propagation - Table 3.1. See Section 3.3 for further discussion).

3.2.3 MCA as model analysis tool

Thus far we focused on MCA of characteristics of the AP in the HH-model and its link to experimentation. Specifically for larger models, MCA can be an important tool for model analysis. In addition to quantifying the contribution of each of the processes to the model behaviour it can also help in understanding the role of the processes. This is most clearly illustrated for

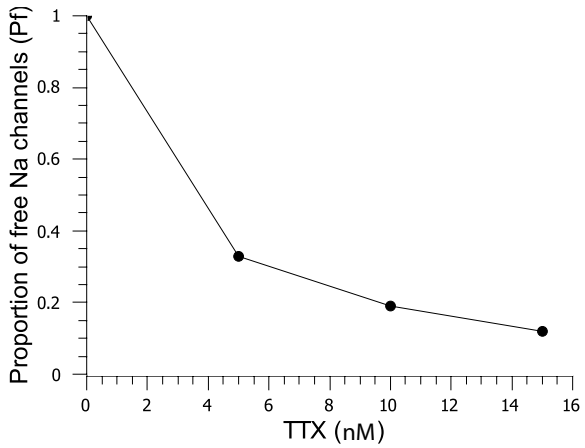

(a)

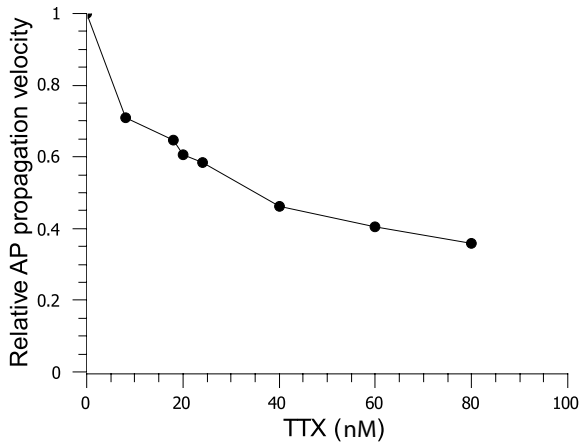

(b)

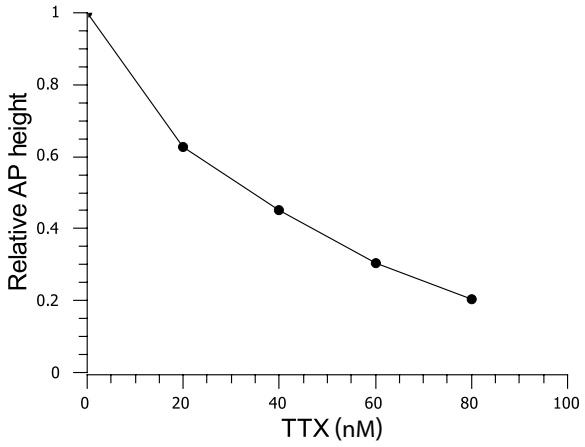

(c)

Figure 3.3: The effect of the addition of Tetrodotoxin on the proportion of free Na channels (p_f), AP propagation speed and the AP height (peak). The degree of Na channel blocking (a) is more pronounced compared to the AP propagation speed slowing (b) or decrease in AP height (c), as the speed and height are dependent on more than the Na channels alone. In the model the effect of TTX is depicted by decreasing $\bar{G}_{Na}$. Data shown in (a) was taken from[161] and data shown in (b) and (c) taken from[162].

steady-state systems, where the control coefficients can be expressed in terms of elasticity coefficients, thereby making it possible to relate system properties to characteristics of the isolated processes. For dynamic systems such an analysis has not been made, but MCA can still be an important tool for the analysis of models for such systems. The approach that we follow here, progression control analysis, has been developed in our group and was illustrated for an oscillatory and a transient system[75]. Recently we used the approach for a control analysis of the restriction point in the eukaryotic cell cycle[190]. For the analysis the control coefficients for each process are determined at fixed points in the progression of the signal and in this way the summation theorems still hold. The control coefficients for the variables of the HH-model during the progression through the AP are shown in Fig. 3.4 for n, m and h and in Fig. 3.5 for the membrane potential (V). The values for the control coefficients vary strongly during the action potential with a switch in sign at the peak of the respective variable. The control coefficients have large values, reflecting the high responsiveness of the system: at time points where the variables change rapidly the control values are large. The summation theorems hold at each time point, i.e. the sum of the control coefficients for each variable add up to zero. The distribution of the process control coefficient profiles[†] is similar for the V, m, and n variables while the control profile distribution for the h variable is inversed. The control profiles are also somewhat similar in shape as the m, h and V variables have two distinctive peaks. This might seem strange as the variables are not directly linked to one another. In metabolic pathways the intermediates of the pathway are linked via mass transfer through chemical reactions, but that is not the case in the HH-model; in principle m, n and h could be independent. On closer inspection of the rate equations, however, it becomes evident that the α and β rate constants for m, n and h are functions of the membrane potential. Thus, each perturbation leading to a change in membrane potential will indirectly change m, n and h. In turn, these changes in m, n and h affect the ion channel conductivity and thereby the ion currents and the membrane potential. This loop structure, where an initial perturbation of the membrane potential leads to a further perturbation of the membrane potential, forms the basis for the generation of the AP.

The intricate linking of all variables to the membrane potential via feedback

[†]Process control coefficient profile refers to the shape of the graph as represented by the dynamic control coefficients determined throughout a percentage progression (see Fig. 3.4 as example).

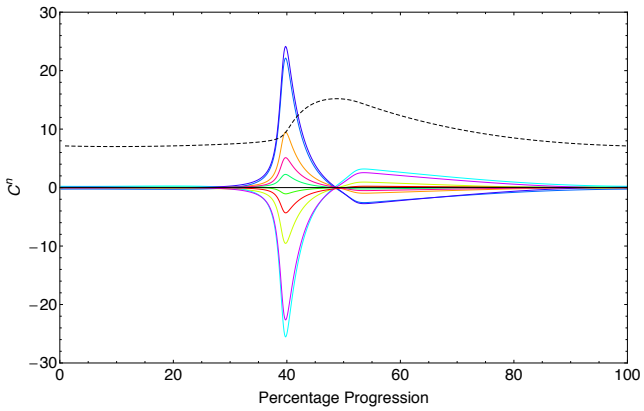

(a)

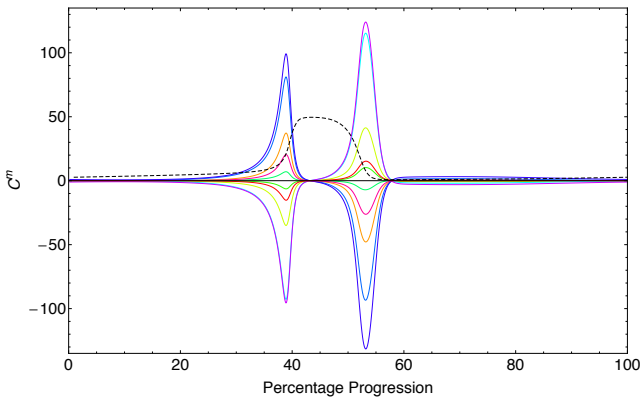

(b)

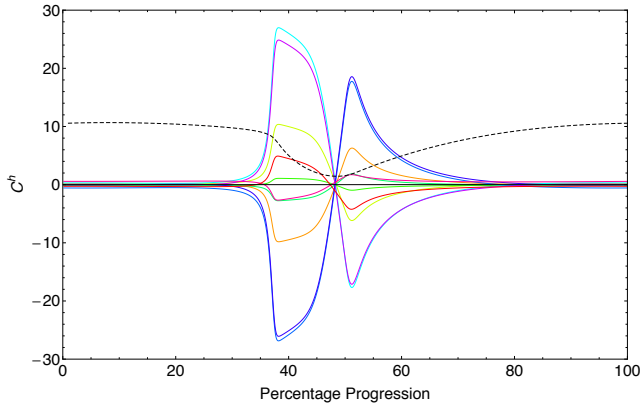

(c)

Figure 3.4: Progression control profiles of the model processes on system variables n (3.4a), m (3.4b) and h (3.4c). The respective variables are indicated by the dashed lines and have been scaled by a factor of 20 for the sake of visual clarity. Control coefficients are shown for each process at points throughout the progression of the respective variable (comparable to the progression of the AP). Legend of the model processes are as indicated in Fig. 3.5.

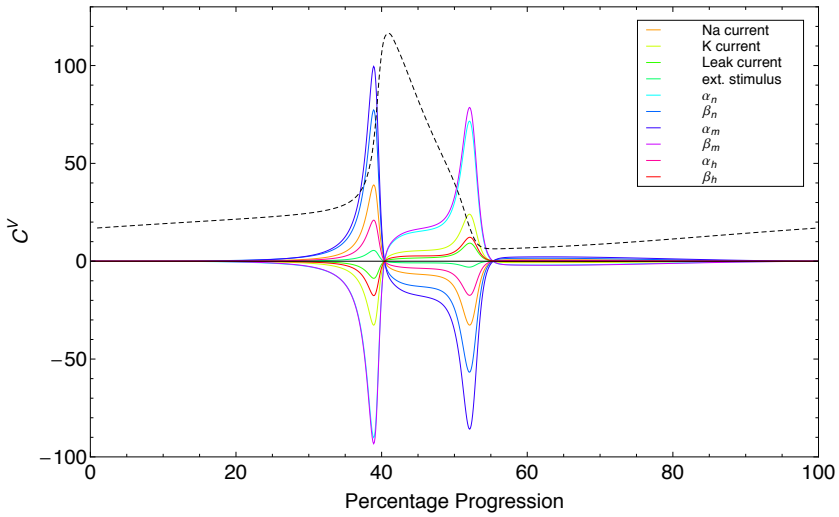

Figure 3.5: Progression control profile of the model processes on system variable V. The variable V is indicated by the dashed line and has an offset of $+77\,\mathrm{mV}$. The voltage offset was chosen to maintain V at a positive value to avoid artificial divergences due to the formalism of MCA in the calculation of the control coefficients. Control coefficients are shown for each process at points throughout the progression of the AP.

loops, makes it complicated to unravel the contribution of the individual processes to the system behaviour. Nonetheless, such an analysis is possible through model simulation. We demonstrate the mechanism of feedback via V on the control profile of α_n on n. The control profile of α_n on n indicates an overall negative control, which is counterintuitive since the model description indicates that an increase in α_n increases n. In overview, the effect of an increase in α_n, increases n and the K current, causing a decrease in V. This initial decrease in V feeds back to the rate constants of all the gating particles affecting their currents which in turn again affects the V and α_n (as our example investigates the effect of α_n). If we want to understand this counterintuitive control, we have to unravel the contributions of the feedback loops. In order to do this, we need to analyse the system as a hierarchical network, where local systems (termed components) for n, m and h are connected via V, analysing the system on five consecutive levels. The simulation results in Fig. 3.6 show the relative contribution of the different component feedback loops in determining the global effect of α_n on n.

First, the local effect of the perturbation is determined at a clamped voltage (*Voltage Clamped*) so as to result in the direct effect of α_n on n only. In the next analysis, the K current decreases the V which feeds back to and decreases α_n and increases β_n; this effect is reflected in the difference in the voltage clamped and *K current (n)* component control profiles, as the *K current (n)* profile causes the effect on n to be decreased by the feedback effect. The next analysis considers the *Na current (m)* component, which decreases in response to the initial decrease in V, in turn further decreasing (via a decrease in V) the effect of α_n on n. This effect is reflected in the large negative component, decreasing the effect of α_n on n even more. Next, the *Na current (h)* is considered. The initial decrease in V results in an increase in *Na current (h)* component ($\epsilon_V^{\beta_h} \ll 0$), increasing (via an increase in V) the effect of α_n on n. This is reflected in the large positive component indicating an increase in the effect of α_n on n. Lastly, the remaining contribution to the control profile of α_n on n is from the positive component of the *Leak current*. These four current components, including the local effect of α_n on n, added together give the total *Combined currents* effect of α_n on n (Fig. 3.6).

We have here indicated a way through which we can determine the contribution/importance of the individual feedback loop components of the HH-model in causing the observed systems behaviour.

3.3 Discussion

The mechanism behind the AP generation and propagation is well known: the involvement of Na and K ion channels underlying the shifts in Na and K ion concentrations which are responsible for the behaviour and shape of the AP is well understood. Through the years, these and other channels (such as calcium) have been characterised and a multitude of channel families identified. The great variety in ion channel types in differing types of neurons, implies a range of channel kinetics underlying observed neuronal behaviour. The AP characteristics of the HH-model and analyses done on this model, are a representation of the channel dynamics of the squid axon. Many modifications have been made to the original HH-model in order to describe more complex neuronal behaviour. The HH-model is one of the most well-known and well-studied models in neuroscience. Despite this, the relative contributions of the model processes to the system behaviour have not been quantified. The mathematical framework we used for this analysis is MCA, which entails the

perturbation of system processes. The HH-model is well suited for the use of MCA as the model is divided into distinct biological processes, which can be perturbed. The combination of model and analysis tool deepened our mechanistic understanding of the model and the mechanisms behind the observed neuronal behaviour by allowing us to determine, both qualitatively and quantitatively, the role of the processes in the observed neuronal behaviour.

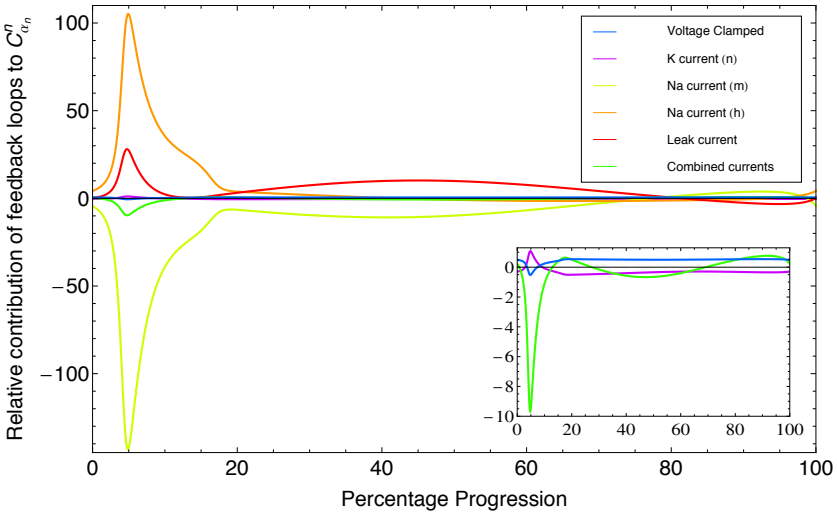

Figure 3.6: Relative feedback loop contribution to the progression profile of $C^n_{\alpha_n}$. The contribution of specific components (as indicated in the legend) were determined through model simulation. In each case, (except for the *Voltage clamped* component), the effect of the V feedback on $C^n_{\alpha_n}$ of the specified component only, was determined. A negative component contributes to decrease the profile of $C^n_{\alpha_n}$, whereas a positive component has a positive contribution to the profile. The combined effect of the loops are shown as *Combined currents*. The inset is a magnification of the vertical axis to show the relatively small *Voltage Clamped*, *K current (n)* and *Combined currents* components.

In our analysis we determined on which of the AP properties MCA can be performed and quantified the control of the model processes on the AP height, threshold, firing frequency and propagation speed for which the control coefficients summed up to either 0 or 1. From the steady-state analysis of the AP properties, we could identify patterns in process controls. For instance, any process that would cause an increase in Na current (i.e. $\bar{G}_{Na}$, α_m, α_h), would also cause the AP threshold to lower, and the peak, propagation

speed and firing frequency to increase, in general, amplifying the AP. The opposite pattern could be seen for the K channel. The strength of MCA, when compared to traditional approaches such as sensitivity analysis, lies in process perturbation: in MCA the processes of the system are perturbed. This makes it possible to link the perturbation of model processes with experimental perturbation. For instance, it has been shown experimentally that TTX increases the neuronal firing threshold by reducing the number of working Na channels[188,189] and has a significant effect on the neuronal firing pattern[191]. This corresponds with our model analysis as the CC of the Na current on the threshold and firing frequency indicates that a decrease in Na current causes the threshold to increase and firing frequency to decrease (Table 3.1). As the control coefficients indicate (Table 3.1), it is not only the qualification of process controls but also the quantification that makes MCA powerful.

We were able to express relations between the system properties (CCs) and process properties (elasticity coefficients). We used these relations, together with inhibitor titrations (taken from literature), to calculate the control of the Na channel on AP height and propagation speed and compared it with our model simulation. Although the control coefficients calculated from the experiments ($C_{\bar{G}_{Na}}^{\text{AP peak}}$ and $C_{\bar{G}_{Na}}^{\text{propagation speed}}$) do not compare very well with those from the model simulation, they are still qualitatively the same. The quantitative discrepancy is perhaps not too surprising, since the HH-model is a core model and does not have a very detailed system description. Even more so, the tissue that was used to determine the response coefficients ($R_{TTX}^{\text{propagation speed}}$ and $R_{TTX}^{\text{AP height}}$), was the rabbit desheathed vagus nerve as opposed to the squid giant axon and might account for the quantitative difference in control coefficients.

Apart from quantifying the controls on steady-state system properties, we also determined the dynamic control profiles of each system process on the variables in the system; n, m, h and V. The dynamic profiles were very similar suggesting that the seemingly distinct variables (n, m and h) are in fact linked. This proves to be the case as the α and β rate constants, directly affecting the m, n and h variables, are all functions of the membrane potential. As an example of elucidating the role by the different feedback mechanisms, we used the high, counterintuitive negative control of α_n on n. We determined the relative contribution of the different feedback loops via V which are responsible for the observed resultant behaviour upon a process perturbation, as per our example, the perturbation effect of α_n on n (Fig. 3.6).

Apart from the loop contribution illustrated in Fig. 3.6, we also determined the contribution as a percentage of the global effect of α_n on n. In order to take into account the total effect of the loop throughout the progression profile, we used the integral of the specific components as it gives a more accurate account of the total effect of α_n on n for the specific loop. We used the integral for the complete system (the *Combined currents*) as the reference value and normalised this to 100%. Note that this integral has a negative value: the overall effect of increasing α_n on n is negative, a counterintuitive effect. Subsequently we expressed the contribution of each of the loops relative to this reference value. The *Voltage Clamped* component has a contribution of -132% of the *Combined currents*, indicating that α_n has an overall positive effect on n in the *Voltage Clamped* system. Considering the *K current (n)* component, it has a contribution of 84% of the *Combined currents*. This suggests that the overall positive effect of α_n on n for the local *Voltage Clamped* system is changed to a negative effect if the feedback loop of V is added to the system. The next component, *Na current (m)*, has a large contribution of 3404% of the *Combined currents*. This component would serve to decrease the effect of α_n on n to a great extent. Considering the *Na current (h)* component, it has a contribution of -1841% of the *Combined currents* and thus has the opposite effect of the *Na current (m)* component. Similarly, the *Leak current* component has the opposite effect of the *Na current (m)* component, with a contribution of -1415% of the *Combined currents*. Together, the *Na current (m)* and *Leak current* components largely cancel the effect of the *Na current (m)* component. It is evident that where the relatively large components would cause a dramatic change in the effect of α_n on n, they cancel each other out to a great extent so that most of the observed global effect is brought about by the K current feedback.

To the best of our knowledge, our method of model analysis resulting in the qualitative and quantitative prediction of neuronal behaviour upon process perturbation of the original HH-model has not been done. Through dynamic progression control analysis we could elicit a deeper understanding of the HH-model system and consequently determine the relative contribution of the feedback loops to the effect of a perturbation in the system. In addition, our work provides a form of integration between the fields of SB and neuroscience by using a SB tool (MCA) to analyse the processes controlling high-level neuronal behaviour and gain further understanding of the HH-model.

3.4 Methods

3.4.1 Action potential

Much of our understanding of the ionic mechanisms responsible for the initiation and propagation of the AP comes from studies on the squid giant axon by A. L. Hodgkin and A. F. Huxley in 1952. HH derived a set of differential equations with which they were able to model the properties of the AP with remarkable accuracy (Figs 3.1 and 3.2)[1].

3.4.2 Extended models

Currently many models exist that incorporate many biological processes in order to present the most accurate description of biological phenomena possible. For neuronal models this might include a diverse array of Na and K channel families or Ca channels or describe more complex neuronal signalling through the use of branched systems.

3.4.3 The Hodgkin-Huxley model

Despite its simplistic nature, the HH-model (created in 1952) provides a fairly accurate description of the AP and AP propagation and is still widely used as a more simplistic model to describe neuronal behaviour. To establish the HH-model, they used certain key experimental methods including a space and voltage clamp[1]. They also measured individual ionic currents and determined which ions were involved in the phases of the AP. Clamping the voltage allowed them to measure ionic currents quantitatively. Their model is an empirical approach to the kinetic description of excitable membranes and accurately predicts the properties of APs. The HH-model mainly consists of four differential equations. The main equation (Eq. 3.6) describes the membrane as a non-linear electric circuit with I the total membrane current consisting of the capacitive current and the ionic currents. Eqs 3.7-3.9 describe the ion channels

$$I_m(t) = C_m \frac{dV}{dt} + \bar{G}_K n(t)^4 \left[E_K - V(t)\right] + \bar{G}_{Na} m(t)^3 h(t) \left[E_{Na} - V(t)\right] + \bar{G}_{leak} \left[E_{Leak} - V(t)\right] - I_{ext}(t), \tag{3.6}$$

$$\frac{dn}{dt} = f_n V(t) \ [1 - n(t)] - q_n V(t) \, n(t), \tag{3.7}$$

$$\frac{dm}{dt} = f_m V(t) \ [1 - m(t)] - q_m V(t) \, m(t), \tag{3.8}$$

$$\frac{dh}{dt} = f_h V(t) \ [1 - h(t)] - q_h V(t) \, h(t), \tag{3.9}$$

with a gating particle describing the K conductance (n) and two (m - activating and h - inactivating) for Na. The Nernst equation incorporating the reversal potentials is temperature dependent, thus rendering the voltage dependent rate constant functions, f and q, temperature dependent. The constants have been determined at a temperature of 6.3 °C and must be scaled with a Q_{10} of 3 for other temperatures[1]. Eqs 3.10-3.15 describe two rate constants for each of the respective gating particles

$$f_n = 0.01(V + 10)/(\exp \frac{V + 10}{10} - 1), \tag{3.10}$$

$$q_n = 0.125 \exp(V/80), \tag{3.11}$$

$$f_m = 0.1(V + 25)/(\exp \frac{V + 25}{10} - 1), \tag{3.12}$$

$$q_m = 4 \exp(V/18), \tag{3.13}$$

$$f_h = 0.07 \exp(V/20), \tag{3.14}$$

$$q_h = 1/(\exp \frac{V + 30}{10} + 1). \tag{3.15}$$

For reference, the first term of each of the gating particle equations (Eqs 3.7-3.9) will be referred to as rate constants α_n, α_m and α_h respectively, while the second term of each equation will be referred to as rate constants β_n, β_m and β_h respectively.

3.4.4 The propagating action potential

In the case of the propagated AP, Eq. 3.6 can be related to a partial differential equation (PDE). Eqs 3.7, 3.8 and 3.9 remain unchanged. The PDE describing the HH-model AP propagation requires the incorporation of a factor (K) consisting of the radius of the axon $a = 238\ \mu$, the specific resistance of the axoplasm $R_2 = 35.4\ \Omega\,\mathrm{cm}$ and the capacity per unit area of membrane $C_m = 1\ \mu\mathrm{F\,cm^{-2}}$. This leads to the following relation of the membrane current density:

$$I = \frac{a}{2R_2}\,\frac{\partial^2 V}{\partial x^2}, \tag{3.16}$$

with

$$K = \frac{a}{2R_2 C_m} \tag{3.17}$$

and thus

$$\begin{aligned} K\frac{\partial^2 V}{\partial x^2} + \frac{\partial V}{\partial t} = \frac{1}{C_m}\big\{ & -\bar{G}_K n(x,t)^4\,[E_K - V(x,t)] \\ & -\bar{G}_{Na} m(x,t)^3 h(x,t)\,[E_{Na} - V(x,t)] \\ & -\bar{G}_{leak}\,[E_{leak} - V(x,t)] + I_{ext}(x,t)\big\}\,. \end{aligned} \tag{3.18}$$

Eq. 3.6 is thus transformed into Eq. 3.18 (PDE). The HH-model was reconstructed from the original publication[1] using Mathematica 7.0.

3.4.5 Metabolic Control Analysis

In general

$$C^x_{v_i} = \left(\frac{\delta x}{x}\right) / \left(\frac{\delta v_i}{v_i}\right). \tag{3.19}$$

In our model v_i refers to the system processes, consisting of the K-factor, Na current, K current, Leak current, External input, α_n, β_n, α_m, β_m, α_h and β_h. The system properties, referred to as x in Eq. 3.19, include the AP height,

firing threshold, propagation speed and firing frequency. In turn, the value of every system property was determined each time by making an up and down perturbation in the system process to calculate the control coefficient for the specific system process, before continuing to the next process. For example, for the AP height, we perturbed all ten processes to obtain the control coefficient for that specific process on the AP height:

$$C_{\bar{G}_{Na}}^{\text{AP peak}};\ C_{\bar{G}_{K}}^{\text{AP peak}};\ C_{\bar{G}_{Leak}}^{\text{AP peak}}\ \text{etc.}$$

and in the same manner for the firing threshold:

$$C_{\bar{G}_{Na}}^{\text{threshold}};\ C_{\bar{G}_{K}}^{\text{threshold}};\ C_{\bar{G}_{Leak}}^{\text{threshold}}\ \text{etc.}$$

The perturbation size was 0.01% in every case. Thus, it is possible to determine the contribution that each system process has on a specific system property.

When all the steps of a system are simultaneously and equally perturbed, the combined effect of all the changes in system processes on the system properties can be written as the sum of the individual effects caused by each change in a system process. This change in effect can either sum to one or zero. It is thus evident that the respective system processes share the control of a system property and that some processes increase a property while others decrease it. The summation theorems also prove that as conditions change in the system, the distribution of control between the processes will vary within the confines of the summation property.

In a steady-state system the flux control coefficients of all the steps of a metabolic system sum to one and is called the summation property of flux-control coefficients. This can be generalised as

$$\sum_{i=1}^{n} C_i^J = 1, \tag{3.20}$$

where n denotes the number of enzymes in the system. With respect to a steady-state concentration, the control coefficients of all the steps of a metabolic system sum to zero and is called the summation property of concentration-control coefficients. It is generalised as

$$\sum_{i=1}^{n} C_i^s = 0. \tag{3.21}$$

Chapter 4

General discussion

In this thesis the following questions were addressed: 1) Can we apply MCA to the AP and its propagation in the HH-model and if this is possible, 2) what are the qualitative and quantitative contributions of the components of the HH-model in describing the high-level behaviour of the AP?

This chapter will serve as a general discussion and refer to some of the topics discussed throughout the thesis. We start with our approach to MCA of the HH-model, whereafter the link to experimental perturbation and the elucidation of the intricate mechanism of the HH-model is discussed. Following this, whether the HH-model was constructed from a top-down or a bottom-up approach will be addressed. Some ion channel mutations (channelopathies) are then described and compared to model simulation. Lastly, MCA will be used to identify possible drug targets to counter these mutations.

Firstly, to determine if the HH-model lends itself to MCA, we identified all the discernable model components describing the neuronal system (see Section 3.2.1). While the respective ion channel currents were easily distinguishable, we were unsure as to the division of the gating particle equations. The particles, m, n and h do not have a mechanistic interpretation, but determine the state of the ion channels. Such a state can be compared to for instance a phosphorylation state of an enzyme and as such the f and q rate constants could be related to kinases/dephosphatases. However, we termed the two parts of the gating particle equations α and β rate constants and view them as processes, leading to a total of ten components (six α's and β's, three ion channels and the external stimulus). By perturbing all ten components equally, we tested whether the summation theorems held for the system, thus defined. Via the simulations the following theorems were obtained: $\sum_{i=1}^{10} C_i^{\text{AP peak}} = 0$,

$\sum_{i=1}^{10} C_i^{\text{threshold}} = 0$, $\sum_{i=1}^{10} C_i^{\text{firing frequency}} = 1$ and $\sum_{i=1}^{11} C_i^{\text{propagation speed}} = 1$. The results of this analysis, as discussed in Chapter 3, indicate that we can apply MCA and we successfully quantified the control of the model components on the following system properties: AP height, threshold, propagation speed and firing frequency.

This also allowed our analysis to be extended to experimental work as distinctive components are used in experimental perturbations. Through the use of experimental inhibitor titrations from literature, we could calculate the control of the sodium channel on AP characteristics and compare it with control coefficients derived from our model simulation. We also determined the dynamic control profiles of the model components on the system variables. The similar control profiles of the system variables led to further investigation, resulting in the identification and quantification of different feedback loops via the membrane potential when effecting a component perturbation. The linking of all the system variables to one another via the membrane potential is indicative of the intricate feedback loops in the HH-model (and the biological system).

A model can be constructed using a bottom-up or top-down approach or even a combination of both, as is often the case. In their experiments, HH used the voltage clamp technique to measure changes in ionic conductance and identified both ionic species responsible for the mechanism behind the AP, namely sodium and potassium. With these measurements they constructed their model, which could reproduce the observed behaviour of the AP. This would indicate that they used a bottom-up approach. In addition, they could validate their model with the observed behaviour of the AP, which their model reproduced. At the time, however, membrane ion channels were not known to exist; HH were not able to use the specific kinetic characteristics of the ion channels, but rather only observed the changes in conductance, i.e. constructing the model equations by fitting them onto the observed ionic conductances. Thus one can argue that it was a top-down approach to model construction. Top-down approaches usually coincide with a hypothesised mechanism of the action of the system if the exact mechanism is not known. In this case, HH hypothesised a mechanism of ion channel gating. Interestingly, their equations of the mechanistic description of the sodium and potassium channel gating particles coincide with the number of respective biological channel subunits (see Eqs 2.20 and 2.21). We propose that it comes down to a matter of perspective, depending on the definition of component data

and observed model behaviour; we are inclined to believe that observed conductance changes and high-level behaviour (such as AP propagation speed) are further removed from one another than (unknown) channel characteristics and the related observed conductance changes. Therefore, although we might see the HH-model as a combination of approaches, we believe it to be constructed more from a bottom-up approach, as opposed to top-down. In general, it is becoming more feasible to construct models using a bottom-up approach, as a wealth of component data has become available in the last couple of years due to advances in measurement technology, for instance.

In neuroscience, these advances mean that many of the mechanisms behind the so-called channelopathies that lead to pathological behaviour of the AP, such as epilepsy, have been characterised in literature. It has been shown that one of the general mechanisms responsible for this behaviour is a decrease in firing threshold resulting in an increase in firing frequency.

Considering the Na channel mutations, an increase in Na channel activation and a decrease in Na channel inactivation specifically lead to a decrease in threshold. From the MCA results, our model predicts that an increase in Na activation (increase in α_m) will decrease the firing threshold ($C_{\alpha_h}^{\text{threshold}} = -6.078$; Table 3.1). On the other hand, a decrease in Na inactivation (increase in α_h) will decrease the firing threshold ($C_{\alpha_m}^{\text{threshold}} = -0.670$; Table 3.1). Both these predictions correspond with experimental results of the mutations as discussed in Chapter 2 (Section 2.7)[184].

Considering the K channel mutation, it has been shown that a reduction in K current leads to the decrease in firing threshold and consequent increase in firing frequency. Once again, our model indicates a decrease in K current would result in a decrease in threshold ($C_{\bar{G}_K}^{\text{threshold}} = 2.401$; Table 3.1), i.e. also corresponding with experimental results[183].

Shifting focus to the firing frequency, our model predictions of the Na activation particle on the firing frequency, shows an increase in activation leading to an increase in frequency ($C_{\alpha_m}^{\text{frequency}} = 1.491$; Table 3.1). Also, a decrease in Na inactivation (increase in α_h) leads to an increase in frequency ($C_{\alpha_h}^{\text{frequency}} = 0.291$; Table 3.1), corresponding with experimental results[184]. Considering the K channel, a decrease in K conductance will lead to an increase in firing frequency ($C_{\bar{G}_K}^{\text{frequency}} = -0.623$; Table 3.1) and is also experimentally supported (Section 2.7)[172,173]. All our simulation results correspond well with the changes caused by the mentioned mutations.

Given that the physiological effect of mutations is known, together with our

quantification of the biological neuronal component control on AP behaviour, we went a step further to pinpoint drug targets. Considering the SCN2A (L1563V) mutation as example, the control profile of the firing frequency suggests various possible targets that could counteract the change caused by the mutation. In view of the physiological result of the mutation (increase in firing frequency), an intuitive counter-target would be one that has a high control on the frequency, such as a decrease in Na current through the Na channel or an increase in K current through the K channel (Table 3.1). Pharmacological studies confirm that drugs such as Lignocaine and Phenytoin act by blocking the Na current and are effective anti-epileptic drugs (AEDs)[192]. Considering the KCNQ2/3 mutation, the control profile of the firing frequency suggests an intuitive counter-action to the increase in frequency to be an increase in K current through the K channel, or a decrease in Na current through the Na channel. K channel openers, like Retigabine, have been shown to be an effective agent in increasing K current through the channel and is an effective AED in treating benign familial neonatal infantile syndrome (BFNIS)[193–195].

As an illustration of the results of the mutations and subsequent treatment with AEDs, AP firing frequency profiles were simulated for the L1563V and R21W mutations (results not shown). When a continuous stimulus of 12 mV is introduced, a normal (unperturbed) AP firing frequency of 0.1903 Hz is produced. When mimicking the L1563V mutation (inserting a linear multiplier in the equation which describes the Na activation) causing an increase in Na activation (for instance 10% increase), there is a 14.91% increase in firing frequency (increased to 0.2187 Hz). Countering these effects by perturbing an identified "drug target", would require a 26.37% decrease in $\bar{G}_{Na}$ resulting in a 12.98% decrease in frequency, returning to 0.1903 Hz. Also, when mimicking the R214W mutation (inserting a linear multiplier in the term describing the K conductance) causing a decrease in K conductance, (again 10% decrease), there is a 6.23% increase in firing frequency (increased to 0.2021 Hz). Perturbing the counter "drug target" to counter this effect would require a 9.41% increase in $\bar{G}_K$) resulting in a 5.86% decrease in frequency, returning to a normal frequency of 0.1903 Hz. Apart from the qualitative aspects, the power of our analysis lies in the quantitative prediction of these drug targets to counter the effects of toxins or mutations. If one were to determine the extent of inhibition of one of the components, for instance via an inhibition titration (as reported for TTX inhibition of $\bar{G}_{Na}$), one could calculate the concentration of drug that

would be needed to counter a specific disease pattern.

We performed MCA on the AP and its properties and compared the control of the Na channel on the AP peak and propagation speed of our model simulation to that of experimental work. We used dynamic progression control analysis to elicit a deeper understanding of the HH-model system and consequently quantified the relative contribution of the feedback loops to the effect of a perturbation in the system. Through our model analyses, we have managed to bring the two separate fields of computational neuroscience and SB closer together by using MCA, a SB tool to analyse one of the oldest and most widely used models in neuroscience.

Lastly, in terms of future work, this analysis approach can be applied to any model that lends itself to MCA (as discussed in this thesis). Naturally, if this analysis were to be performed on a model with a more detailed biological description, the quantitative predictions would be even more valuable than that obtained from the HH model. A more detailed neuronal model coupled with the quantitative framework of MCA could be especially important to counter a specific disease pattern or toxin.

Bibliography

1. Hodgkin, A. L., and Huxley, A. F. (1952) A quantitative description of membrane current and its application to conduction and excitation in nerve. *Journal of Physiology 117*, 500–544.

2. Ashcroft, F. M. *Ion channels and disease: channelopathies*; Academic Press: Boston, 2000.

3. Lehmann-Horn, F., and Jurkat-Rott, K. (1999) Voltage-gated ion channels and hereditary disease. *Physiological Review 79*, 1317–1372.

4. Bower, J. In *Computational modeling of genetic and biochemical networks*; Bower, J. M., and Bolouri, H., Eds.; MIT Press: Cambridge, MA, 2001.

5. De Schutter, E. (2008) Why are Computational Neuroscience and Systems Biology So Separate? *PLOS Computational Biology 4*, 1–6.

6. Kotaleski, J. H., and Blackwell, K. T. (2010) Modelling the molecular mechanisms of synaptic plasticity using systems biology approaches. *Nature Revviews Neuroscience 11*, 239–251.

7. Bruggeman, F. J., and Westerhoff, H. V. (2007) The nature of systems biology. *Trends in Microbiology 15*, 45–50.

8. Kacser, H., and Burns, J. A. (1973) The control of flux. *Symposia of the Society for Experimental Biology 27*, 65–104.

9. Heinrich, R., and Rapoport, T. A. (1974) A linear steady-state treatment of enzymatic chains. General properties, control, effector strength. *European Jounal of Biochemistry 42*, 89–95.

10. Heinrich, R., and Rapoport, T. A. (1975) Mathematical analysis of multienzyme systems. II. Steady state and transient control. *BioSystems 7*, 130–136.

11. Wiener, N. *Cybernetics - Control and Communication in the Animal and the Machine*; John Wiley and Sons: New York, 1948.

12. Levchenko, A. (2001) Computational cell biology in the post-genomics era. *Molecular Biology Reports 28*, 83–89.

13. Mesarovic, M. D. *Systems theory and biology*; Springer Verlag: Berlin, 1968.

14. Bertalanffy, L. V. *General Systems Theory*; George Braziller: New York, 1968.

15. Savageau, M. A. (1969) Biochemical systems analysis. I. Some mathematical properties of the rate law for the component enzymatic reactions. *Journal of Theoretical Biology 25*, 365–369.

16. Savageau, M. A. (1969) Biochemical systems analysis. II. The steady-state solutions for an n-pool system using a power-law approximation. *Journal of Theoretical Biology 25*, 370–379.

17. Kitano, H. *Foundations of Systems Biology*; MIT Press: Cambridge, MA, 2001; pp xiii–xv.

18. Ideker, T., Thorsson, V., Ranish, J. A., Christmas, R., Buhler, J., Eng, J. K., Bumgarner, R., Goodlett, D. R., Aebersold, R., and Hood, L. (2001) Integrated genomic and proteomic analyses of a systematically perturbed metabolic network. *Science 292*, 929–934.

19. Hood, L., Ideker, T., and Galitski, T. (2001) A new approach to decoding life: Systems biology. *Annual Review of Genomics and Human Genetics 2*, 343–372.

20. Kitano, H. (2002) Systems biology: A brief overview. *Science 295*, 1662–1664.

21. Barkai, N., and Leibler, S. (1997) Robustness in simple biochemical networks. *Nature 387*, 913–917.

22. Alon, U., Surette, M. G., Barkai, N., and Leibler, S. (1999) Robustness in bacterial chemotaxis. *Nature 397*, 168–171.

23. Yi, T. M., Huang, Y., Simon, M. I., and Doyle, J. (2000) Robust perfect adaptation in bacterial chemotaxis through integral feedback control. *Proceedings of the National Academy of Science USA 97*, 4649–4653.

24. Kitano, H. (2003) Cancer robustness: tumour tactics. *Nature 426*, 125.

25. Kitano, H. (2004) Cancer as a robust system: implications for anticancer therapy. *Nature Reviews Cancer 4*, 227–235.

26. Kitano, H. (2004) Biological robustness. *Nature Review Genetics 5*, 826–837.

27. von Dassow, G., Meir, E., Munro, E. M., and Odell, G. M. (2000) The segment polarity network is a robust developmental module. *Nature 406*, 188–192.

28. ldar, A., Dorfman, R., Weiss, D., Ashe, H., Z., S. B., and Barkai, N. (2002) Robustness of the BMP morphogen gradient in Drosophila embryonic patterning. *Nature 419*, 304–308.

29. Meir, E., von Dassow, G., Munro, E., and Odell, G. M. (2002) Robustness, flexibility, and the role of lateral inhibition in the neurogenic network. *Current Biology 12*, 778–786.

30. Schlosser, G., and Wagner, G. *Modularity in Development and Evolution*; The University of Chicago Press: Chicago, 2004.

31. Schlichting, C., and Pigliucci, M. *Phenotypic Evolution: A Reaction Norm Perspective*; Sinauer Associates, Inc.: Sunderland, 1998.

32. Agrawal, A. A. (2001) Phenotypic plasticity in the interactions and evolution of species. *Science 294*, 321–326.

33. Huck, M., Finney, A., Sauro, H. M., Bolouri, H., Doyle, J. C., and Kitano, H. (2003) The systems biology markup language (SBML): a medium for representation and exchange of biochemical network models. *Bioinformatics 19*, 524–531.

34. Shapiro, B. E., Finney, A., Hucka, M., Bornstein, B., Funahashi, A., Jouraku, A., Keating, S. M., Le Novère, N., Matthews, J., and Schilstra, M. J. In *Introduction to Systems Biology*; Sangdun, C., Ed.; Humana Press Inc.: Totowa, New Jersey, 2007; Chapter SBML Models and MathSBML, pp 395–421.

35. Kitano, H., Funahashi, A., Matsuoka, Y., and Oda, K. (2005) Using process diagrams for the graphical representation of biological networks. *Nature Biotechnology 23*, 961–966.

36. Le Novère, N. et al. (2005) Minimal information requested in the annotation of models (MIRIAM). *Nature Biotechnology 23*, 1509–1515.

37. Keseler, I. M., Collado-Vides, J., Gama-Castro, S., Ingraham, J., Paley, S., Paulsen, I. T., Peralta-Gil, M., and Karp, P. D. (2005) EcoCyc: a comprehensive database resource for Escherichia coli. *Nucleic Acids Research 33*, D334–D337.

38. Olivier, B., and Snoep, J. L. (2004) Web-based kinetic modelling using JWS Online. *Bioinformatics 20*, 2143–2144.

39. Salgado, H., Gama-Castro, S., Martínez-Antonio, A., Díaz-Peredo, E., Sánchez-Solano, F., Peralta-Gil, M., Garcia-Alonso, D., Jiménez-Jacinto, V., Santos-Zavaleta, A., Bonavides-Martínez, C., and Collado-Vides, J. (2004) RegulonDB (version 4.0): transcriptional regulation, operon organization and growth conditions in Escherichia coli K-12. *Nucleic Acids Research 32*, D303–D306.

40. Le Novère, N., Bornstein, B., Broicher, A., Courtot, M., Donizelli, M., Dharuri, H., Li, L., Sauro, H., Schilstra, M., Shapiro, B., Snoep, J. L., and Hucka, M. (2006) BioModels database: a free, centralized database of curated, published, quantitative kinetic models of biochemical and cellular systems. *Nucleic Acids Research 34*, D689–D691.

41. Förster, J., Famili, I., Fu, P., Palsson, B. Ø., and Nielsen, J. (2003) Genome-scale reconstruction of the Saccharomyces cerevisiae metabolic network. *Genome Research 13*, 244–253.

42. Ma, H. W., and Zeng, A. P. (2003) Reconstruction of metabolic networks from genome data and analysis of their global structure for various organisms. *Bioinformatics 19*, 270–277.

43. Herrgard, M. J., Covert, M. W., and Palsson, B. O. (2004) Reconstruction of microbial transcriptional regulatory networks. *Current Opinion in Biotechnology 15*, 70–77.

44. Papin, J. A., Hunter, T., Palsson, B. O., and Subramaniam, S. (2005) Reconstruction of cellular signalling networks and analysis of their properties. *Nature Reviews Molecular Cell Biology 6*, 99–111.

45. Ma, H. W., da Silva, M. R., Sun, J. B., Kumar, B., and Zeng, A. P. In *Introduction to Systems Biology*; Sangdun, C., Ed.; Humana Press Inc.: Totowa, New Jersey, 2007; Chapter Reconstruction and Structural Analysis of Metabolic and Regulatory Networks, pp 124–146.

46. Overbeek, R., Larsen, N., Pusch, G. D., D'Souza, M., Selkov, E. J., Kyrpides, N., Fonstein, M., Maltsev, N., and Selkov, E. (2000) WIT: integrated system for high-throughput genome sequence analysis and metabolic reconstruction. *Nucleic Acids Research 28*, 123–125.

47. Karp, P. D., Riley, M., Saier, M., Paulsen, I. T., Paley, S. M., and Pellegrini-Toole, A. (2000) The EcoCyc and MetaCyc databases. *Nucleic Acids Research 28*, 56–59.

48. Kanehisa, M., Goto, S., Kawashima, S., Okuno, Y., and Hattori, M. (2004) The KEGG resource for deciphering the genome. *Nucleic Acids Research D277-D280*, 32.

49. Edwards, J. S., and Palsson, B. O. (2000) The Escherichea coli MG1655 in silico metabolic genotype: its definition, characteristics, and capabilities. *Proceedings of the National Academy of Science USA 97*, 5528–5533.

50. Becker, S. A., and Palsson, B. O. (2005) Genome-scale reconstruction of the metabolic network in Staphylococcus aureus N315: an initial draft to the two-dimensional annotation. *BMC Microbiology 5*, 8.

51. Thiele, I., Vo, T. D., Price, N. D., and Palsson, B. Ø. (2005) Expanded metabolic reconstruction of Helicobacter pylori (iIT341 GSM/GPR): an in silico genome-scale characterization of single- and double-deletion mutants. *Journal of Bacteriology 187*, 5818–5830.

52. Yu, H., Luscombe, N. M., Lu, H. X., Zhu, X., Xia, Y., Han, J. D., Bertin, N., Chung, S., Vidal, M., and Gerstein, M. (2004) Annotation transfer between genomes: protein-protein interologs and protein-DNA regulogs. *Genome Research 14*, 1107–1118.

53. Makita, Y., Nakao, M., Ogasawara, N., and Nakai, K. (2004) DBTBS: database of transcriptional regulation in Bacillus subtilis and its contribution to comparative genomics. *Nucleic Acids Research 32*, D75–D77.

54. Münch, R., Hiller, K., Barg, H., Heldt, D., Linz, S., Wingender, E., and Jahn, D. (2003) PRODORIC: prokaryotic database of gene regulation. *Nucleic Acids Research 31*, 266–269.

55. Matys, V. et al. (2003) TRANSFAC: transcriptional regulation, from patterns to profiles. *Nucleic Acids Research 31*, 374–378.

56. Herrgard, M. J., Lee, B., Portnoy, V., and Palsson, B. Ø. (2006) Integrated analysis of regulatory and metabolic networks reveals novel regulatory mechanisms in Saccharomyces cerevisiae. *Genome Res. 16*, 627–635.

57. Yeger-Lotem, E., Sattath, S., Kashtan, N., Itzkovitz, S., Milo, R., Pinter, R. Y., Alon, U., and Margalit, H. (2004) Network motifs in integrated cellular networks of transcription-regulation and protein-protein interaction. *Proceedings of the National Academy of Science USA 20*, 5934–5939.

58. Ma, H. W., Buer, J., and Zeng, A. P. (2004) Hierarchical structure and modules in the Escherichia coli transcriptional regulatory network revealed by a new top-down approach. *BMC Bioinformatics 5*, 199–208.

59. Ma, H. W., Kumar, B., Ditges, U., Gunzer, F., Buer, J., and Zeng, A. P. (2004) An extended transcriptional regulatory network of Escherichia coli and analysis of its hierarchical structure and network motifs. *Nucleic Acids Research 32*, 6643–6649.

60. Ideker, T., Galitski, T., and Hood, L. (2001) A new approach to decoding life: systems biology. *Annual Review of Genomics and Human Genetics 2*, 343–372.

61. Hood, L., Heath, J. R., Phelps, M. E., and Biaoyang, L. (2004) Systems biology and new technologies enable predictive and preventative medicine. *Science 306*, 640–643.

62. Oliveira, A. P., Jewett, M. C., and Nielsen, J. In *Introduction to Systems Biology*; Sangdun, C., Ed.; Humana Press Inc.: Totowa, New Jersey, 2007; Chapter From Gene Expression to Metabolic Fluxes, pp 37–66.

63. Churchill, G. A. (2002) Fundamentals of experimental design for cDNA microarrays. *Nature Genetics 32*, 490–495.

64. Quackenbush, J. (2002) Microarray data normalization and transformation. *Nature Genetics 32*, 496–501.

65. Eisen, M. B., Spellman, P. T., Brown, P. O., and Botstein, D. (1998) Cluster analysis and display of genome-wide expression patterns. *Proceedings of the National Academy of Science USA 95*, 14863–14868.

66. Ideker, T., Ozier, O., Schwikowski, B., and Siegel, A. F. (2002) Discovering regulatory and signalling circuits in molecular interaction networks. *Bioinformatics 18*, S233–S240.

67. Patil, K. R., and Nielsen, J. (2005) Uncovering transcriptional regulation of metabolism by using metabolic network topology. *Proceedings of the National Academy of Sciences USA 102*, 2685–2689.

68. Reijenga, K. A., van Megen, Y. M. G. A., Kooi, B. W., Bakker, B. M., Snoep, J. L., van Verseveld, H. W., and Westerhoff, H. V. (2005) Yeast glycolytic oscillations that are not controlled by a single oscillophore: a new definition of oscillophore strength. *Journal of Theoretical Biology 232*, 385–398.

69. Acerenza, L., Sauro, H. M., and Kacser, H. (1989) Control analysis of time-dependent metabolic systems. *Journal of Theoretical Biology 137*, 423–444.

70. Kholodenko, B. N., Demin, O. V., and Westerhoff, H. V. (1997) Control analysis of periodic phenomena in biological systems. *Journal of Physical Chemistry B 101*, 2070–2081.

71. Demin, O. V., Westerhoff, H. V., and Kholodenko, B. N. (1999) Control analysis of stationary forced oscillations. *Journal of Physical Chemistry 103*, 10695–10710.

72. Heinrich, R., and Reder, C. (1991) Metabolic control analysis of relaxation processes. *Journal of Theoretical Biology 151*, 343–350.

73. Acerenza, L. In *Control of Metabolic Processes*; Cornish-Bowden, A., and Cardenas, M. L., Eds.; Plenum Press: New York, 1990; Chapter Temporal aspects of the control of metabolic processes, pp 297–302.

74. Acerenza, L., and Kacser, H. (1990) Enzyme kinetics and metabolic control. A method to test and quantify the effect of enzymic properties on metabolic variables. *Biochemical Journal 269*, 697–707.

75. Conradie, R., Westerhoff, H. V., Rohwer, J. M., Hofmeyr, J. S., and Snoep, J. L. (2006) Summation theorems for flux and concentration control coefficients of dynamic systems. *IEE Proceedings Systems Biology 153*, 314–317.

76. De Schutter, E. In *Computational neuroscience: realistic modeling for experimentalists*; De Schutter, E., Ed.; CRC Press: Boca Raton, FL, 2000; p 348.

77. Sejnowski, T. J., Koch, C., and Churchland, P. S. (1988) Computational neuroscience. *Science 241*, 1299–1306.

78. Steuber, V., Mittmann, W., Hoebeek, F. E., Silver, R. A., De Zeeuw, C. I., Häusser, M., and De Schutter, E. (2007) Cerebellar LTD and pattern recognition by Purkinje cells. *Neuron 54*, 121–136.

79. Le Novère, N. (2007) The long journey to a Systems Biology of neuronal function. *BMC Systems Biology 1*, 28.

80. De Schutter, E., Ascoli, G. A., and Kennedy, D. N. (2006) On the future of the human brain project. *Neuroinformatics 4*, 129–130.

81. Gershenfeld, N. *The Nature of Mathematical Modelling*; Cambridge University Press, 1998.

82. Eykhoff, P. *System Identification: Parameter and State Estimation*; John Wiley & Sons, 1974.

83. Aldridge, B. B., Burke, J. M., Lauffenburger, D. A., and Sorger, P. K. (2006) Physicochemical modelling of cell signalling pathways. *Nature Cell Biology 8*, 1195–1203.

84. Raj, A., and van Oudenaarden, A. (2008) Nature, Nurture, or Chance: Stochastic Gene Expression and Its Consequences. *Cell 135*, 216–226.

85. Morris, M. K., Saez-Rodriguez, J., Sorger, P. K., and Lauffenburger, D. A. (2010) Logic-Based Models for the Analysis of Cell Signaling Networks. *Biochemistry 49*, 3216–3224.

86. Balicki, J. (2004) Multi-criterion Evolutionary Algorithm with Model of the Immune System to Handle Constraints for Task Assignments. *Artificial Intelligence and Soft Computing 3070*, 394–399.

87. Lee, H. Y., Topham, D. J., Park, S. Y., Hollenbaugh, J., Treanor, J., Mosmann, T. R., Jin, X., Ward, B. M., Miao, H., Holden-Wiltse, J., Perelson, A. S., Zand, M., and Wu, H. (2009) Simulation and Prediction of the Adaptive Immune Response to Influenza A Virus Infection. *Journal of Virology 83*, 7151–7165.

88. McIntosh, R. *The Background of Ecology. Concept and Theory.*; Cambridge University Press: New York, 1985.

89. Lotka, A. J. *Elements of Physical Biology*; Williams and Wilkins, 1925.

90. Volterra, V. (1926) Variazioni e fluttuazioni del numero d'individui in specie animali conviventi. *Memoirs dei Accademia Reale Nazionale dei Lincei Ser VI 2*.

91. Bronfenbrenner, U. (1977) Toward an experimental ecology of human development. *American Psychologist 32*, 512–1531.

92. Bronfenbrenner, U. *The Ecology of Human Development: Experiments by Nature and Design*; Harvard University Press: Cambridge, MA, 1979.

93. Hawley, A. H. *Human ecology: A theory of community structure.*; New York: Ronald Press., 1950.

94. Moore, J. F. *The Death of Competition: Leadership & Strategy in the Age of Business Ecosystems*; Harper Business: New York, 1996.

95. Churchland, P. S., Koch, C., and Sejnowski, T. S. In *Computational Neuroscience*; Schwartz, E. L., Ed.; MIT Press, 1993; Chapter What is computational neuroscience?, pp 46–55.

96. Lapicque, L. (1907) Recherches quantitatives sur l'excitation électrique des nerfs traitée comme une polarisation. *Journal of Physiology, Pathology and Genetics 9*, 620–635.

97. Brunel, N., and Van Rossum, M. C. (2007) Lapicque's 1907 paper: from frogs to integrate-and-fire. *Biological Cybernetics 97*, 337–339.

98. Hubel, D. H., and Wiesel, T. N. (1962) Receptive fields, binocular interaction and functional architecture in the cat's visual cortex. *Journal of Physiology 160*, 106–54.

99. Marr, D. (1969) A theory of cerebellar cortex. *Journal of Physiology 202*, 437–470.

100. Marr, D. (1971) Simple memory: a theory for archicortex. *Philosophical Transactions of the Royal Society London 262*, 23–81.

101. Marr, D. (1975) Approaches to biological information processing. *Science 190*, 875–876.

102. Wu, S., and Johnston, D. *Foundations of cellular neurophysiology.*; MIT Press.: Cambridge, MA, 1995.

103. Koch, C. *Biophysics of computation: information processing in single neurons.*; Oxford University Press, 1999.

104. Chklovskii, D. B., Mel, B. W., and Svoboda, K. (2004) Cortical rewiring and information storage. *Nature 431*, 782–788.

105. Barlow, H. B. (1961) Possible principles underlying the transformation of sensory messages. *Sensory Communication* 217–234.

106. Hebb, D. O. *The organization of behavior*; Wiley: New York, 1949.

107. Hopfield, J. J. (1982) Neural networks and physical systems with emergent collective computational abilities. *Proceedings of the National Academy of Sciences of the USA 79*, 2554–2558.

108. Durstewitz, D., Seamans, J. K., and Sejnowski, T. J. (2000) Neurocomputational models of working memory. *Nature Neuroscience 3*, 1184–1191.

109. Fusi, S., Drew, P. J., and Abbott, L. F. (2005) Cascade models of synaptically stored memories. *Neuron 45*, 599–611.

110. Coggan, J. S., Bartol, T. M., Esquenazi, E., Stiles, J. R., Lamont, S., Martone, M. E., Berg, D. K., Ellisman, M. H., and Sejnowski, T. J. (2005) Evidence for ectopic neurotransmission at a neuronal synapse. *Science 309*, 446–451.

111. Aisa, B., Mingus, B., and O'Reilly, R. (2008) The emergent neural modeling system. *Neural networks 21*, 1146–1152.

112. Adorjan, P., Barna, G., Erdi, P., Grobler, T., Kepecs, A., Lengyel, M., and Ventriglia, F. (1996) Multicompartmental modeling of hippocampal pyramidal cells and interneurons with the GENESIS software tool. *Neurobiology 4*, 247–249.

113. Gewaltig, M., and Diesmann, M. (2007) NEST (NEural Simulation Tool). *Scholarpedia 2*, 1430.

114. Migliore, M., Cannia, C., Lytton, W. W., Markram, H., and Hines, M. L. (2006) Parallel network simulations with NEURON. *Journal of Computational Neuroscience 21*, 119–129.

115. Gleeson, P., Steuber, V., and Silver, R. A. (2007) neuroConstruct: A Tool for Modeling Networks of Neurons in 3D Space. *Neuron 54*, 219–235.

116. Davison, A. P., Brüderle, D., Eppler, J. M., Kremkow, J., Muller, E., Pecevski, D. A., Perrinet, L., and Yger, P. (2008) PyNN: a common interface for neuronal network simulators. *Frontiers in Neuroinformatics 2*, 1–10.

117. Cornelis, H., and De Schutter, E. (2003) Neurospaces: Separating modeling and simulation. *Neurocomputing 52*, 227–231.

118. Markram, H. (2006) The blue brain project. *Nature Reviews Neuroscience 7*, 153–160.

119. FitzHugh, R. (1961) Impulses and Physiological States in Theoretical Models of Nerve Membrane. *Biophysical Journal 1*, 445–466.

120. FitzHugh, R. *Mathematical models of excitation and propagation in nerve.*; McGraw-Hill Book Co.: New York, 1969; Chapter 1, pp 1–85.

121. Morris, C., and Lecar, H. (1981) Voltage oscillations in the barnacle giant muscle fiber. *Biophysical Journal 35*, 193–213.

122. Hindmarsh, J. L., and Rose, R. M. (1984) A model of neuronal bursting using three coupled first order differential equations. *Proceedings of the Royal Society London 221*, 87–102.

123. Fox, R. F. (1997) Stochastic Versions of the Hodgkin-Huxley Equations. *Biophysical Journal 72*, 2068–2074.

124. Tanaka, H., and Aihara, K. (2004) Analysis of the Hodgkin-Huxley equations with noise: the effects of noise on chaotic neurodynamics. *Artificial Life and Robotics 8*, 190–196.

125. Austin, T. D. (2008) The emergence of the deterministic Hodgkin-Huxley equations as a limit from the underlying stochastic ion-channel mechanism. *Annals of Applied Probability 18*, 1279–1325.

126. Schmid, G., Goychuk, I., and Hanggi, P. (2004) Controlling the spiking activity in excitable membranes via poisoning. *Physica A 344*, 665–670.

127. Gong, Y., Xu, B., Ma, X., and Han, J. (2008) Effect of channel block on the collective spiking activity of coupled stochastic Hodgkin-Huxley neurons. *Science in China, Series B: Chemistry 51*, 341–346.

128. Strassberg, A. F., and DeFelice, L. J. (1993) Limitations of the Hodgkin-Huxley Formalism: Effects of Single Channel Kinetics on Transmembrane Voltage Dynamics. *Neural Computation 5*, 843–655.

129. Ginzburg, S. L., and Pustovoit, M. A. (2006) Response of Hodgkin-Huxley stochastic bursting neuron to single-pulse stimulus. *Physica A 369*, 354–368.

130. Moehlis, J. (2006) Canards for a reduction of the Hodgkin-Huxley equations. *Journal of Mathematical Biology 52*, 141–153.

131. Cressman, J. R., Ullah, G. J., Ziburkus, J., Schiff, S., and Barreto, E. (2009) The influence of sodium and potassium dynamics on excitability, seizures, and the stability of persistent states: I. Single neuron dynamics. *Journal of Computational Neuroscience 26*, 159–170.

132. Ullah, G., Cressman, J. R., Barreto, E., and Schiff, S. J. (2009) The influence of sodium and potassium dynamics on excitability, seizures, and the stability of persistent states: II. Network and glial dynamics. *Journal of Computational Neuroscience 26*, 171–183.

133. Yam, Y., and Lo, C. (2007) A mathematical model for potassium channel conductance in Hodgkin-Huxley experiments. *Proceedings of the American Control Conference* 2726–2731.

134. Carter, B. C., and Bean, B. P. (2009) Sodium Entry during Action Potentials of Mammalian Neurons: Incomplete Inactivation and Reduced Metabolic Efficiency in Fast-Spiking Neurons. *Neuron 64*, 898–909.

135. Seyama, I., and Irisawa, H. (1967) The Effect of High Sodium Concentration on the Action Potential of the Skate Heart. *The Journal of General Physiology 50*, 505–517.

136. Fridlyand, L. E., Jacobson, D. A., Kuznetsov, A., and Philipson, L. H. (2009) A Model of Action Potentials and Fast Ca2 Dynamics in Pancreatic beta-Cells. *Biophysical Journal 96*, 3126–3139.

137. Shen, G. Y., Chen, W. R., Midtgaard, J., Shepherd, G. M., and Hines, M. L. (1999) Computational Analysis of Action Potential Initiation in Mitral Cell Soma and Dendrites Based on Dual Patch Recordings. *Journal of Neurophysiology 82*, 3006–3020.

138. Majumdar, S., and Sikdar, S. K. (2007) Periodicity in Na+ channel properties alters excitability of a model neuron. *Biochemical and Biophysical Research Communications 359*, 908–914.

139. Anderson, W. S., Kudela, P., Cho, J., Bergey, G. K., and Franaszczuk, P. J. (2007) Studies of stimulus parameters for seizure disruption using neural network simulations. *Biological Cybernetics 97*, 173–194.

140. Fohlmeister, J. F. (2009) A nerve model of greatly increased energy-efficiency and encoding flexibility over the Hodgkin-Huxley models. *Brain Research 1296*, 225–233.

141. Raymond, S. A. (1992) Subblocking Concentrations of Local Anesthetics: Effects on Impulse Generation and Conduction in Single Myelinated Sciatic Nerve Axons in Frog. *Anesthesia & Analgesia 75*, 906–921.

142. Keynes, R. D., Ritchie, J. M., and Rojas, E. (1971) The binding of tetrodotoxin to nerve membranes. *Journal of Physiology 213*, 235–254.

143. Schwaber, J. S., Graves, E. B., and Paton, J. F. R. (1993) Computational modeling of neuronal dynamics for systems analysis: application to neurons of the cardiorespiratory NTS in the rat. *Brain Research 604*, 126–141.

144. Li, H., Che, Y., Gao, H., Dong, F., and Wang, J. (2008) Bifurcation analysis of the Hodgkin-Huxley model exposed to external DC electric fields. *22nd IEEE International Symposium on Intelligent Control, ISIC 2007. Part of IEEE Multi-conference on Systems and Control* 271–276.

145. McIntyre, C. C., and Grill, W. M. (1998) Sensitivity analysis of a model of mammalian neural membrane. *Biological Cybernetics 79*, 29–37.

146. Huang, C. W., Tsai, J. J., Huang, C. C., and Wu, S. N. (2009) Experimental and simulation studies on the mechanisms of levetiracetam-mediated inhibition of delayed-rectifier potassium current (KV3.1): Contribution to the firing of action potentials. *Journal of physiology and pharmacology 60*, 37–47.

147. Khodorov, B. I., Timin, Y. N., Vilenkin, S. Y., and Gul'ko, F. B. (1970) Theoretical analysis of the mechanisms of conduction of a nerve impulse along an inhomogeneous axon II. Conduction of a single impulse across a region of the fibre with modified functional properties. *Biophysics 15*, 145–152.

148. Adair, R. K. (2004) Optimum ion channel properties in the squid giant axon. *Physical Review E 69*, 42902–42904.

149. Sangrey, T. D., Friesen, W. O., and Levy, W. B. (2004) Analysis of the Optimal Channel Density of the Squid Giant Axon Using a Reparameterized Hodgkin-Huxley Model. *Journal of Neurophysiology 91*, 2541–2550.

150. Crotty, P., Sangrey, T., and Levy, W. B. (2006) Metabolic Energy Cost of Action Potential Velocity. *Journal of Neurophysiology 96*, 1237–1246.

151. Jin, W., Xu, J., Wu, Y., and Rui, Z. (2004) Controlling Neuronal Spike by Ion Channels with Weak Periodic Perturbation. *Proceedings of the 5th World Congress on Intelligent Control and Automation* 5347–5340.

152. Chavarette, F. R., Balthazar, J. M., Rafikov, M., and Hermini, H. A. (2009) On non-linear dynamics and an optimal control synthesis of the action potential of membranes (ideal and non-ideal cases) of the Hodgkin-Huxley (HH) mathematical model. *Chaos, Solitons and Fractals 39*, 1651–1666.

153. Fei, X., Wang, J., and Chen, L. (2006) Bifurcation control of Hodgkin-Huxley model of nerve system. *Proceedings of the World Congress on Intelligent Control and Automation (WCICA) 2*, 9406–9410.

154. Wang, J., Chen, L., and Fei, X. (2007) Analysis and control of the bifurcation of Hodgkin-Huxley models. *Chaos, Solitons and Fractals 31*, 247–256.

155. Cessac, B., and Samuelides, M. (2007) From neuron to neural networks dynamics. *European Physical Journal Special Topics 142*, 7–88.

156. Wang, J., Chen, L., and Fei, X. (2007) Bifurcation control of the Hodgkin-Huxley equations. *Chaos, Solitons and Fractals 33*, 217–224.

157. Xie, Y., Chen, L., Kang, Y. M., and Aihara, K. (2008) Controlling the onset of Hopf bifurcation in the Hodgkin-Huxley model. *Physical Review E 77*, 061921.

158. Calitoiu, D., Oommen, B. J., and Nussbaum, D. (2008) Spikes annihilation in the Hodgkin-Huxley neuron. *Biological Cybernetics 98*, 239–257.

159. Borkowski, L. S. (2009) Response of a Hodgkin-Huxley neuron to a high-frequency input. *Physical Review E 80*, 051914.

160. Nakamura, Y., Nakajima, S., and Grundfest, H. (1965) The Action of Tetrodotoxin on Electrogenic Components of Squid Giant Axons. *The Journal of General Physiology 48*, 985–996.

161. Cuervo, L. A., and Adelman, W. J. (1970) Equilibrium and kinetic properties of the interaction between tetrodotoxin and the excitable membrane of the squid giant axon. *Journal of General Physiology 55*, 309–335.

162. Colquhoun, D., and Ritchie, J. M. (1972) The interaction at equilibrium between tetrodotoxin and mammalian non-myelinated nerve fibres. *Journal of Physiology 221*, 533–553.

163. Keynes, R. D., Greeff, N. G., Forster, I. C., and Bekkers, J. M. (1991) The effect of tetrodotoxin on the sodium gating current in the squid giant axon. *Proceedings of the Royal Society London B 246*, 135–140.

164. Crotty, P., and Levy, W. B. (2007) Effects of Na+ channel inactivation kinetics on metabolic energy costs of action potentials. *Neurocomputing 70*, 1652–1656.

165. Shapiro, B. I., and Lenherr, F. K. (1972) Hodgkin-Huxley axon increased modulation and linearity of response to constant current sitimulus. *Biophysical Journal 12*, 1145–1158.

166. Migliore, M., Morse, T. M., Davison, A. P., Marenco, L., Shepherd, G. M., and Hines, M. L. (2003) ModelDB: making models publicly accessible to support computational neuroscience. *Neuroinformatics 1*, 135–139.

167. Lehmann-Horn, F., and Rüdel, R. (1997) Channelopathies: Their contribution to our knowledge about voltage-gated ion channels. *News in Physiological Sciences 12*, 105–112.

168. Lewis, T. B., Shevell, M. I., Andermann, E., Ryan, S. G., and Leach, R. J. (1996) Evidence of a third locus for benign familial convulsions. *Journal of Child Neurology 11*, 211–214.

169. Heron, S. E., Crossland, K. M., Andermann, E., Phillips, H. A., Hall, A. J., Bleasel, A., Shevell, M., Mercho, S., Seni, M. H., Guiot, M. C., Mulley, J. C., Berkovic, S. F., and Scheffer, I. E. (2002) Sodium-channel defects in benign familial neonatalinfantile seizures. *Lancet 360*, 851–852.

170. Yang, Y., Beyer, B. J., Otto, J. F., O'Brien, T. P., Letts, V. A., White, H. S., and Frankel, W. N. (2003) Spontaneous deletion of epilepsy gene orthologs in a mutant mouse with a low electroconvulsive threshold. *Human Molecular Genetics 12*, 975–984.

171. Otto, J. F., Yang, Y., Frankel, W. N., Wilcox, K. S., and White, H. S. (2004) Mice Carrying the Szt1 Mutation Exhibit Increased Seizure Susceptibility and Altered Sensitivity to Compounds Acting at the M-Channel. *Epilepsia 45*, 1009–1016.

172. Schroeder, B. C., Kubisch, C., Stein, V., and Jentsch, T. J. (1998) Moderate loss of function of cyclic-AMP-modulated KCNQ2/KCNQ3 K+ channels causes epilepsy. *Nature 396*, 687–690.

173. Otto, J. F., Yang, Y., Frankel, W. N., White, H. S., and Wilcox, K. S. (2006) A Spontaneous Mutation Involving Kcnq2 (Kv7.2) Reduces M-Current Density and Spike Frequency Adaptation in Mouse CA1 Neurons. *The Journal of Neuroscience 26*, 2053–2059.

174. Reid, C. A., Berkovic, S. F., and Petrou, S. (2009) Mechanisms of human inherited epilepsies. *Progress in Neurobiology 87*, 41–57.

175. Brown, D. A., and Adams, P. R. (1980) Muscarinic suppression of a novel voltage-sensitive K+ current in a vertebrate neurone. *Nature 283*, 673–676.

176. Halliwell, J. V., and Adams, P. R. (1982) Voltage-clamp analysis of muscarinic excitation in hippocampal neurons. *Brain Research 250*, 71–92.

177. Rundfeldt, C., and Netzer, R. (2000) The novel anticonvulsant retigabine activates M-currents in Chinese hamster ovary-cells tranfected with human KCNQ2/3 subunits. *Neuroscience Letters 282*, 73–76.

178. Main, M. J., Cryan, J. E., Dupere, J. R. B., Cox, B., Clare, J. J., and Burbidge, S. A. (2000) Modulation of KCNQ2/3 Potassium Channels by the Novel Anticonvulsant Retigabine. *Molecular Pharmacology 58*, 253–262.

179. McDonough, J. H., and Shih, T. (1997) Neuropharmacological Mechanisms of Nerve Agent-induced Seizure and Neuropathology. *Neuroscience & Biobehavioral Reviews 21*, 559–579.

180. Hamilton, S. E., Loose, M. D., Qi, M., Levey, A. I., Hille, B., McKnight, G. S., Idzerda, R. L., and Nathanson, N. M. (1997) Disruption of the m1 receptor gene ablates muscarinic receptor-dependent M current regulation and seizure activity in mice. *Proceedings of the National Academy of Science USA 94*, 13311–13316.

181. Brown, D. A., Gähwiler, B. H., Griffith, W. H., and Halliwell, J. V. (1990) Membrane currents in hippocampal neurons. *Progress in Brain Research 83*, 141–60.

182. Rogawski, M. A. (2000) KCNQ2/KCNQ3 K+ channels and the molecular pathogenesis of epilepsy: implications for therapy. *Trends in Neurosciences 23*, 393–398.

183. Malin, S. A., and Nerbonne, J. M. (2000) Elimination of the Fast Transient in Superior Cervical Ganglion Neurons with Expression of KV4.2W362F: Molecular Dissection of IA. *The Journal of Neuroscience 20*, 5191–5199.

184. Scalmani, P., Rusconi, R., Armatura, E., Zara, F., Avanzini, G., Franceschetti, S., and Mantegazza, M. (2006) Effects in Neocortical Neurons of Mutations of the Nav1.2 Na Channel causing Benign Familial Neonatal-Infantile Seizures. *Neurobiology of Disease 26*, 10100–10109.

185. Giersch, C. (1988) Control analysis of metabolic networks. 1. Homogeneous functions and the summation theorems for control coefficients. *European Journal of Biochemistry 174*, 509–513.

186. Westerhoff, H. V., Aon, M. A., Van Dam, K., Cortassa, S., Kahn, D., and Van Workum, M. (1990) Dynamical and hierarchical coupling. *Biochimica et Biophysica Acta 1018*, 142–146.

187. Reijenga, K. A., Westerhoff, H. V., Kholodenko, B. N., and Snoep, J. L. (2002) Control Analysis for Autonomously Oscillating Biochemical Networks. *Biophysical Journal 82*, 99–108.

188. Takata, M., Moore, J. W., Kao, C. Y., and Fuhrman, F. A. (1966) Blockage of sodium conductance increase in lobster giant axon by tarichatoxin (tetrodotoxin). *Journal of General Physiology 49*, 977–988.

189. Hille, B. (1968) Pharmacological modifications of the sodium channels of frog nerve. *Journal of General Physiology 51*, 199–219.

190. Conradie, R., Bruggeman, F. J., Ciliberto, A., Csikász-Nagy, A., Novák, B., Westerhoff, H. V., and Snoep, J. L. (2010) Restriction point control of the

mammalian cell cycle via the cyclin E/Cdk2:p27 complex. *FEBS Journal 277*, 357–367.

191. Hille, B. *Ionic channels of excitable membranes*; Sinauer Associates Inc., 2001.

192. Schleifer, K. J., Tot, E., and Höltje, H. D. (1998) Pharmacophore and pseudoreceptor modelling of class Ib antiarrhythmic and local anaesthetic lidocaine analogues. *Pharmazie 53*, 596–602.

193. Kapetanovic, I. M., and Rundfeldt, C. (1996) D-23129: A New Anticonvulsant Compound. *CNS Drug Reviews 2*, 308–321.

194. Brown, M. L., Zha, C. C., Van Dyke, C. C., Brown, G. B., and Brouillette, W. J. (1999) Comparative Molecular Field Analysis of Hydantoin Binding to the Neuronal Voltage-Dependent Sodium Channel. *Journal of Medicinal Chemistry 42*, 1537–1545.

195. Rogawski, M. A. (2006) Diverse mechanisms of antiepileptic drugs in the development pipeline. *Epilepsy research 69*, 273–294.